SANDIA REPORT

SAND91-2876 • UC-528
Unlimited Release
Printed October 1997

RSMASS-D Models: An Improved Method for Estimating Reactor and Shield Mass for Space Reactor Applications

Albert C. Marshall

Prepared by
Sandia National Laboratories
Albuquerque, New Mexico 87185 and Livermore, California 94550

Sandia is a multiprogram laboratory operated by Sandia Corporation, a Lockheed Martin Company, for the United States Department of Energy under Contract DE-AC04-94AL85000.

Sandia National Laboratories

SF2900Q(8-81)

Printed in the United States of America. This report has been reproduced directly from the best available copy.

Available to DOE and DOE contractors from
Office of Scientific and Technical Information
P.O. Box 62
Oak Ridge, TN 37831

Prices available from (615) 576-8401, FTS 626-8401

Available to the public from
National Technical Information Service
U.S. Department of Commerce
5285 Port Royal Rd
Springfield, VA 22161

NTIS price codes
Printed copy: A06
Microfiche copy: A01

SAND91-2876
Unlimited Release
Printed October 1997

Distribution
Category UC-528

RSMASS-D MODELS: AN IMPROVED METHOD FOR ESTIMATING REACTOR AND SHIELD MASS FOR SPACE REACTOR APPLICATIONS

Albert C. Marshall
International Nuclear Safety Department
P.O. Box 5800
Sandia National Laboratories
Albuquerque, New Mexico 87185-0744

Abstract

Three relatively simple mathematical models have been developed to estimate minimum reactor and radiation shield masses for liquid-metal-cooled reactors (LMRs), in-core thermionic fuel element (TFE) reactors, and out-of-core thermionic reactors (OTRs). The approach was based on much of the methodology developed for the Reactor/Shield Mass (RSMASS) model. Like the original RSMASS models, the new RSMASS-derivative (RSMASS-D) models use a combination of simple equations derived from reactor physics and other fundamental considerations, along with tabulations of data from more detailed neutron and gamma transport theory computations. All three models vary basic design parameters within a range specified by the user to achieve a parameter choice that yields a minimum mass for the power level and operational time of interest. The impact of critical mass, fuel damage, and thermal limitations are accounted for to determine the required fuel mass. The effect of thermionic limitations are also taken into account for the thermionic reactor models. All major reactor component masses are estimated, as well as instrumentation and control (I&C), boom, and safety system masses. A new shield model was developed and incorporated into all three reactor concept models. The new shield model is more accurate and simpler to use than the approach used in the original RSMASS model. The estimated reactor and shield masses agree with the mass predictions from separate detailed calculations within 15 percent for all three models.

Contents

Contents

Contents

Contents

List of Figures

List of Tables

Acknowledgments

I would like to acknowledge contributions of several individuals. At Sandia National Laboratories, Don Gallup programmed the RSMASS-D models as an algorithm in his systems code and carried out the transport calculations needed to obtain shielding parameters. Gary Harms performed the cross section calculations and Larry Sanchez carried out the calculations for transport theory to obtain the critical mass data used in the thermonic fuel element discussed in this document. François Linet of the French Centre d'Etudes Nucléaires de Saclay and Don King of Sandia compared the RSMASS-D predictions with the results from the detailed mass analysis.

List of Acronyms

ACS	auxiliary core cooling system
DOD	U.S. Department of Defense
DOE	U.S. Department of Energy
FEMP	Finite-element multigroup P_n
GA	General Atomics Technologies
GE	General Electric Company
I&C	instrumentation and control
LMR	liquid-metal-cooled reactor
MMW	multimegawatt
NASA	National Aeronautics and Space Administration
NERVA	nuclear engine for rocket vehicle applications
OTR	out-of-core thermionic reactor
PBR	particle bed reactor
PGC	prismatic core gas-cooled reactor
RSMASS	reactor/shield mass model
RSMASS-D	reactor/shield mass derivative model
SD	smear density
SDI	Strategic Defense Initiative
SNAP	system for nuclear auxiliary power
SPI	Space Power, Inc.
TFE	thermionic fuel element

1. Introduction

1.1 Background

During the mid-1980s, the Strategic Defense Initiative (SDI) Space Power Office of the Department of Defense (DoD) considered a number of reactor systems as electrical power supplies for orbiting defense systems. Since launch costs are a major consideration for any space-based power system, reasonable estimates of the power system masses are essential to identify promising concepts and technologies. Consequently, the Space Power Office requested that Sandia National Laboratories (SNL) develop a simple analytic model capable of making rapid estimates of reactor and shield masses for SDI space reactor power systems. This model was to be used as part of a system mass model and as a separate reactor and shield mass model for parametric studies; the model was also to be used to check mass projections for specific proposed reactor concepts. Since these estimates were to be used to make rough estimates for multimegawatt (MMW) reactor systems, for which the reactor and shield were only a small fraction of the total system mass, a fairly crude model was sufficient to account for the reactor and shield mass contribution. An accuracy goal for the model of a factor of two was chosen.

In response to this request and considering the goals and potential problems with a variety of approaches, an entirely new modeling method was developed and is referred to as the reactor/shield mass (RSMASS) model (Marshall, 1986). Although RSMASS was relatively crude, it exceeded our accuracy goals. More recently, however, greater emphasis has been placed on lower power reactor systems (in the tens to hundreds of kilowatt electric range) for both military and civilian missions. At lower power levels, the reactor and shield make up a larger fraction of the total system mass, and a more accurate reactor and shield mass model is required. Furthermore, the original RSMASS model was somewhat cumbersome to use and could easily be misapplied if it was not used by an experienced nuclear engineer. Finally, the code did not have the capability to automatically optimize the design parameters for the chosen power level, operational time, and other operational choices.

To increase the model's accuracy, simplify its use, and permit automatic mass optimization, a new series of reactor and shield mass models (referred to as the RSMASS-derivative models, or RSMASS-D models) has been developed. The new models build on the successful aspects of the earlier RSMASS model. To simplify the use of the model and permit mass optimization, it became necessary to develop a separate mass model for each type of reactor, rather than using a single model with different parameters for each reactor type. The original shield model was too crude for our new accuracy goals (~20 percent), so an essentially new shield modeling approach was developed.

1.2 RSMASS-D Scope

The RSMASS-D models discussed in this report provide a unique capability for making rapid estimates of space reactor and shield masses. RSMASS-D models have been developed for liquid-metal-cooled reactors (LMRs), thermionic fuel element (TFE) reactors (i.e., in-core thermionic reactors), out-of-core thermionic reactors (OTRs), prismatic core gas-cooled (PGC) reactors, and particle bed reactors (PBRs). At present, only the LMR, TFE reactor, and OTR models have been checked, and only these models are discussed in this document. A separate document that discusses reactor and shield mass models for the PGC and PBR concepts is planned.

Some additional systems that were not present in RSMASS have been added to the RSMASS-D computation. Since the thermionic conversion devices are integral to thermionic reactors, thermionic device mass is also computed. For the out-of-core thermionic reactor, the radiator is an integral part of the reactor system, and its mass is computed as well. A simple relationship is also provided for the payload separation boom mass for all of the models. All three of these models have been incorporated in full power-system models. The system model for the out-of-core thermionic reactor has been documented (Gallup, 1990).

Although the RSMASS-D models are intended to be more accurate than their predecessor (RSMASS), they are still very approximate, and no attempt was made to be rigorous. In fact, some volumetric approximations for the assumed geometry were used instead of exact calculations that would have added some complexity without significantly increasing the accuracy of the mass estimate. Other possible minor mass additions or considerations were also ignored.

1.3 Reference Reactor Power System

The SP-100 LMR was developed for space applications by the Department of Energy (DOE), the National Aeronautics and Space Administration (NASA), and the DoD. The prime contractor for the SP-100 was General Electric Co. (GE). Because the SP-100 is currently the most developed U.S. reactor for space applications, it was chosen as a reference design to guide model development and ensure that all major components were accounted for by reasonable mass estimates in all the models for the various reactor types. For example, the mass of all safety systems, instrumentation and control (I&C), and miscellaneous structure for the TFE reactor and OTR concepts is approximately accounted for by using data from the reference SP-100 design. Furthermore, SP-100 shielding data were used to normalize the shielding equations to obtain reasonable shielding thicknesses for all of the reactor types. The reference SP-100 reactor system data were obtained from two GE documents (GE, 1988a; 1988b) and from discussions with GE staff (Murata, 1988). The reference SP-100 design is for a 100-kWe system using thermoelectric power conversion.

1.4 Calculational Approach

The description of the RSMASS-D calculational approach given here closely follows the presentation in Marshall and Gallup (1991). The calculational flow logic for the LMR, in-core thermionic, and OTR RSMASS-D models is basically the same (see Figure 1-1). The desired power level and reactor operating time, along with other input parameters, are first input to RSMASS-D. Then values for a set of design parameters determined by the design concept being modeled (see Table 1-1) are selected and the reactor subsystem mass is calculated. The values of the set of design parameters are varied through their full range of allowable combinations, and the parameter choice that yields the minimum reactor subsystem mass is selected as the optimized subsystem design.

For each iteration, the fuel mass and the mass of the reactor components are computed. (The fuel mass calculation criteria and the reactor component masses vary according to the design concept; see Table 1-2.) Next, the mass of the ancillary components (also identified in Table 1-2) and the gamma and neutron shields can be computed. The total reactor subsystem mass is the sum of the fuel, reactor-component, ancillary-component, and shield masses.

1.4.1 Liquid-Metal-Cooled Reactors

The LMR model is based on the SP-100 reactor concept (GE, 1988a). The pin diameter, reactor core length-to-diameter ratio, and the fuel cladding gap (Table 1-1) are varied. Using these data and other fixed parameters, the mass of fuel required based on thermal and fuel damage limits is computed. The required critical mass (neutronic-limited critical mass) is obtained using the method developed for RSMASS (Marshall, 1986), modified to include correction factors that are a function of fuel volume fraction and the reactor core length-to-diameter ratio. The actual fuel mass selected is the largest based on neutronic, thermal, and fuel damage considerations. The reactor component masses (structure, reflector, pressure vessel, and

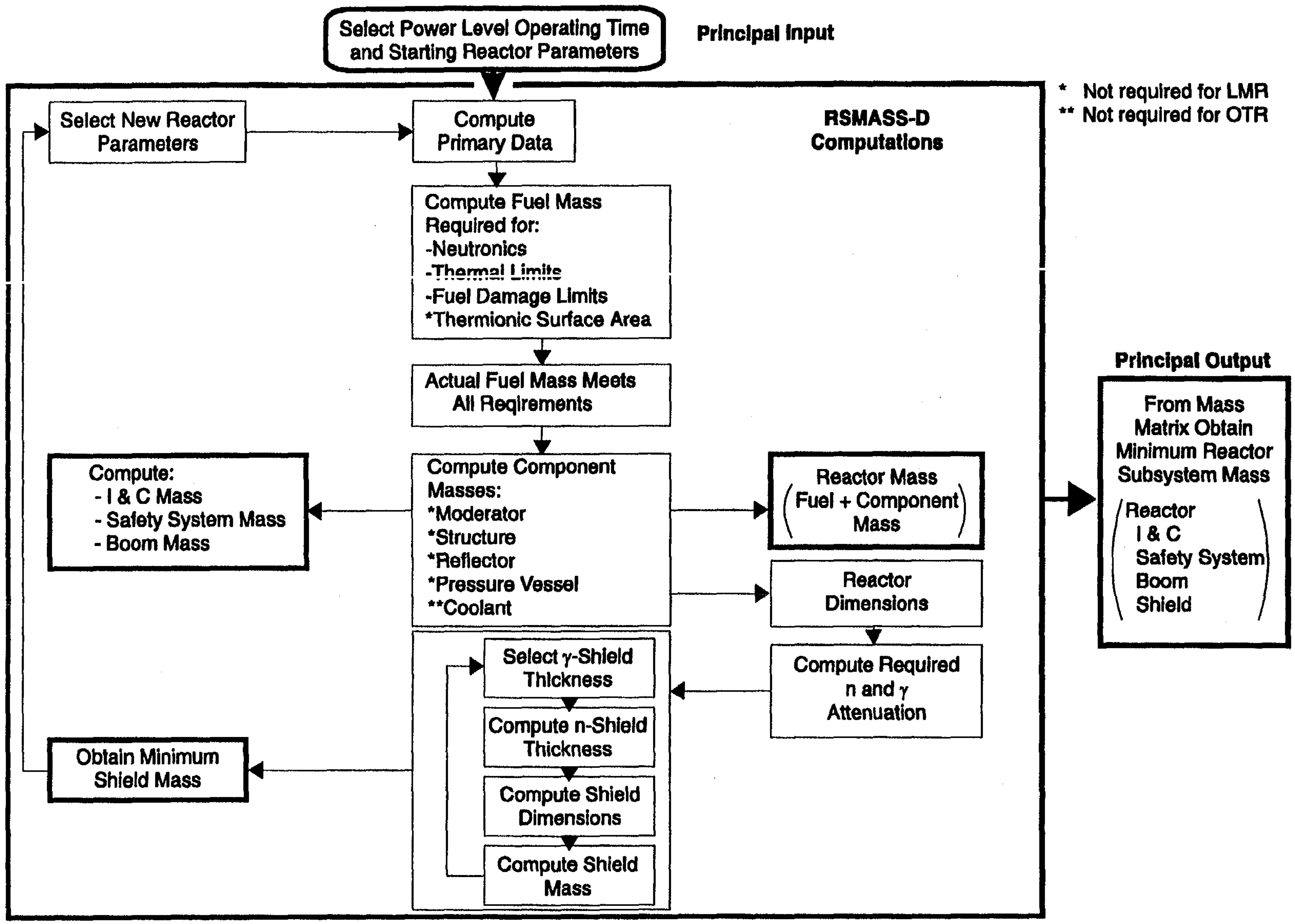

Figure 1-1. RSMASS-D calculational flow diagram.

Table 1-1. Design Parameters Varied in RSMASS-D to Obtain Minimum Reactor Subsystem Mass[a]

Variable Design Parameter	LMR	TFE	OTR
Pin diameter	x		
Reactor core length-to-diameter ratio	x	x	x
Fuel/cladding gap	x		
Thermionic emitter radius		x	
Driver uranium loading		x	
Moderator thickness		x	
Fuel annulus inside/outside diameter			x
Core thermal flux			x
Gamma shield thickness	x	x	x

[a] After Marshall and Gallup (1991)

Table 1-2. RSMASS-D Fuel Calculation Criteria, Reactor Components, and Ancillary Components

Criterion/Component	LMR	TFE	OTR
Fuel Calculation Criterion			
Thermal	x	x	x
Fuel damage	x	x	x
Neutronics	x	x	x
Thermionics		x	x
Reactor Components			
Structure	x	x	x
Reflector	x	x	x
Pressure vessel	x	x	
Coolant	x	x	
Moderator		x	x
Ancillary Components			
I&C	x	x	x
Safety	x	x	x
Boom	x	x	x
Thermionic			x
Radiator			x

coolant) are then computed from the fuel mass and the geometric description of the reactor. Then the total reactor mass (the sum of the fuel mass and component masses) is calculated.

Mass estimates of ancillary components for the LMR are as follows:

- The I&C mass estimate allows for the effects of reactor size, payload separation distance, and other considerations.
- Safety system mass calculations account approximately for auxiliary shutdown (safety) rods, re-entry protection, and other safety-related hardware.
- Boom mass is estimated by assuming a simple linear relationship between boom mass and boom length.

Using the reactor dimensions, the payload separation distance from the reactor, and other information, the required neutron and gamma attenuation is computed. An initial value for the gamma shield thickness is then used with the required attenuation factors to obtain the required neutron shield thickness as predicted by neutron and gamma transport theory calculations. Assuming shadow shield geometry, the shield dimensions and mass are then computed. This process is repeated for other gamma shield thicknesses, and the gamma shield thickness that yields the minimum shield mass is then selected.

1.4.2 In-Core Thermionic Reactors

The in-core thermionic reactor is assumed to consist of thermionic fuel elements (SPI 1987a; GA, 1989). The TFEs may also contain driver fuel pins or a moderator region surrounding the fuel. The TFE model is therefore more complex because all three basic types of TFE reactors must be considered. Nevertheless, the calculation sequence for the in-core thermionic reactor subsystem mass follows the same basic process used for the LMR, with the following exceptions: (1) a different set of design parameters is varied (Table 1-1); (2) the fuel mass based on required thermionic surface area is computed (Table 1-2); and (3) the moderator mass is added to the reactor component calculation (Table 1-2).

1.4.3 Out-of-Core Thermionic Reactors

The OTR model is based on the STAR-C concept proposed by General Atomics (GA, 1987a). The reactor core for this concept consists of a stack of cylindrical graphite trays with a single uranium dicarbide fuel annulus contained within each tray. Heat is transferred through the core by conduction. As with the in-core thermionic reactor, the calculation sequence is similar to that of the LMR, except a different set of design parameters is varied (Table 1-1). In addition, radiator and thermionic masses are calculated for the OTR (Table 1-2).

1.5 Scope and Organization of the Report

To keep this document to a manageable size, some of the correlations used (e.g., for instrumentation, control, and safety subsystem masses) are presented without a lengthy description of their origin. These correlations were based on physical considerations and they provide reasonable mass estimates. The original RSMASS document (Marshall, 1986) should be read first to better understand the discussion of the RSMASS-D models.

This report is organized into four chapters and four appendices.

- Chapter 2 explains the calculational approach for the LMR mass models (Section 2.1), in-core thermionic reactor (Section 2.2), and the OTR (Section 2.3) as well as the calculation procedure for I&C and safety systems.

- Chapter 3 explains the general approach for radiation shield modeling (Section 3.1) and the specific shield models for the LMR (Section 3.2), the in-core thermionic reactor (Section 3.3), and the OTR (Section 3.4); it also presents the calculation procedure for the boom mass.

- Chapter 4 presents results for the 100-kWe LMR and in-core thermionic concepts and the 5 kWe OTR concept (Section 4.1). RSMASS-D results for the three concepts are also compared with detailed calculations (Section 4.2).

- Appendix A provides a derivation of the formula used in RSMASS-D that accounts for the fact that the reactor is a cylinder rather than a sphere, and that the length-to-diameter ratio may exceed 1.

- Appendix B provides recommended values for the input parameters for the three design concepts.

- Appendix C explains the procedure for obtaining the gamma and neutron attenuation coefficients used in Chapter 3.

- Appendix D defines the variables used throughout this report.

1.6 Nomenclature and Unit Conventions

Because RSMASS was originally developed for multimegawatt (MMW) reactors, the unit of power in this document is megawatts. The unit of time is years, dimensional units are in meters, mass units are in kilograms, and thermal conductivity and heat transfer coefficients are W/mK and W/m^2K, respectively. The units for every variable presented in this report are defined in Appendices B and D.

Only the numbered equations (e.g., 2.1-1, 2.1-2, etc.) in this report make up the model algorithms. Equations and expressions containing both numbers and letters (e.g., 3.1-a) are not part of the model algorithms.

2. Reactor Mass Models

The general approach for the reactor model has been discussed, to a large extent, in the RSMASS document (Marshall, 1986). Where the method for this model has not changed from RSMASS, the equations will be provided, but their derivation will not be repeated. Deviations from the original RSMASS model, however, will be discussed in the following sections, and the derivation of equations will be given when appropriate.

2.1 Liquid-Metal-Cooled Reactors

2.1.1 Reactor Description

For the reasons given in Chapter 1, the SP-100 reactor was chosen as the reference design for liquid-metal-cooled reactors. Although the SP-100 reactor was explicitly designed to be used with thermoelectric power conversion, it can be used with a variety of power conversion options (e.g., Stirling, Rankine, Brayton). Some design changes may be required for reactors with high power requirements (e.g., in-core control rods as well as safety rods); nevertheless, the basic SP-100 reactor design should be representative of a whole class of LMRs (without in-core boiling) over a broad reactor power range. LMR designs that permit in-core boiling or use cermet fuel will not be well represented by the model based on the SP-100 design.

The SP-100 reference 100-kWe reactor design is illustrated in Figure 2-1. The reactor core is about 35 cm in length and diameter, and consists of bundles of 0.77-cm-diameter fuel pins contained in a niobium alloy pressure vessel. The fuel pins (Figure 2-2) are made up of uranium nitride fuel pellets within a rhenium-lined niobium alloy cladding. Heat is transferred from the fuel pins to a flowing lithium coolant that carries heat to the power-conversion module. Beryllium oxide reflector segments surround the core circumference and are external to the pressure vessel. The reflector segments are hinged at one end and their radial position is adjusted at the opposite end of the reflector to control reactivity by regulating neutron leakage out of the core. In-core safety rods are also provided to maintain the reactor in a shutdown condition during potential accident scenarios. A graphite reentry heat shield surrounds the reactor to prevent disruption of the core during accidental reentry.

The payload and power system electronics are protected from reactor gamma and neutron radiation by a shadow shield at the aft end of the reactor (Figure 2-3). The shield consists of

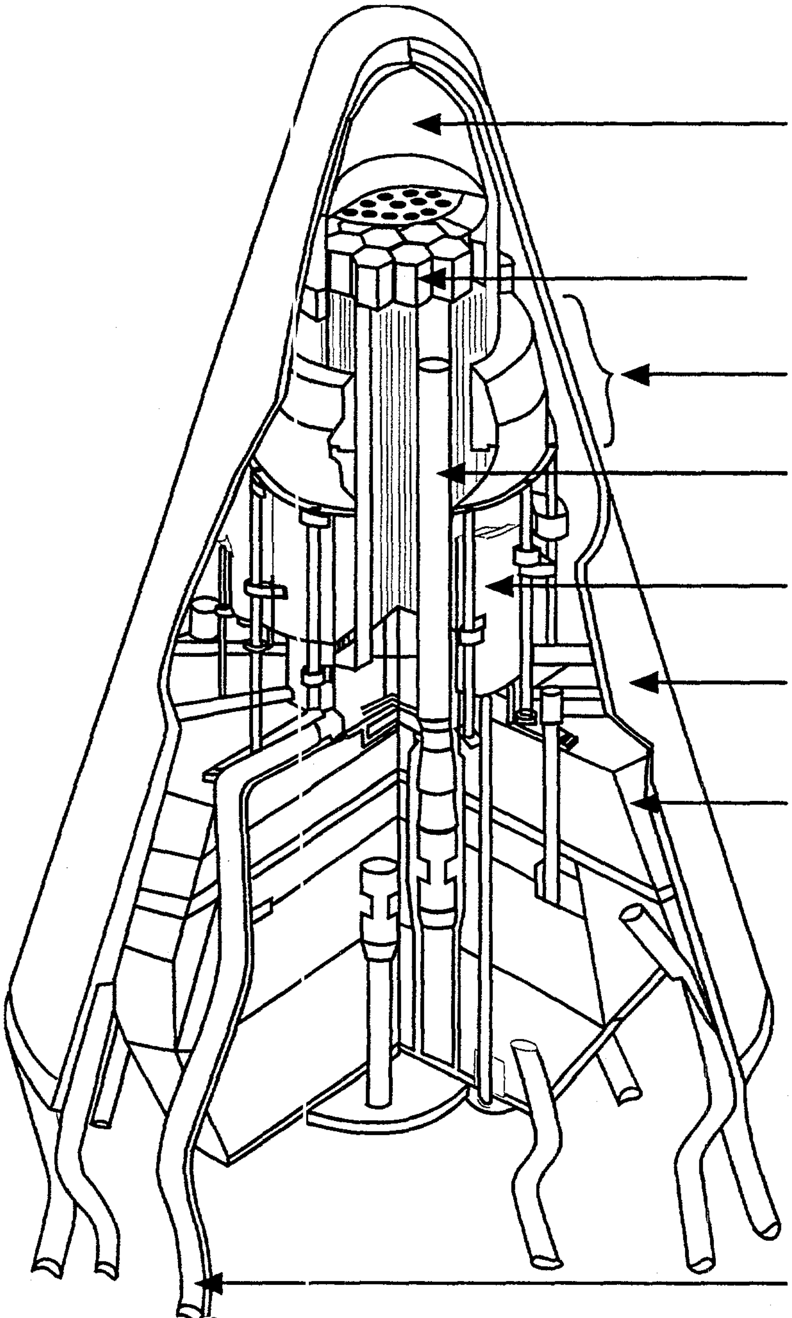

Figure 2-1. SP-100 reactor and shield (GE, 1988b).

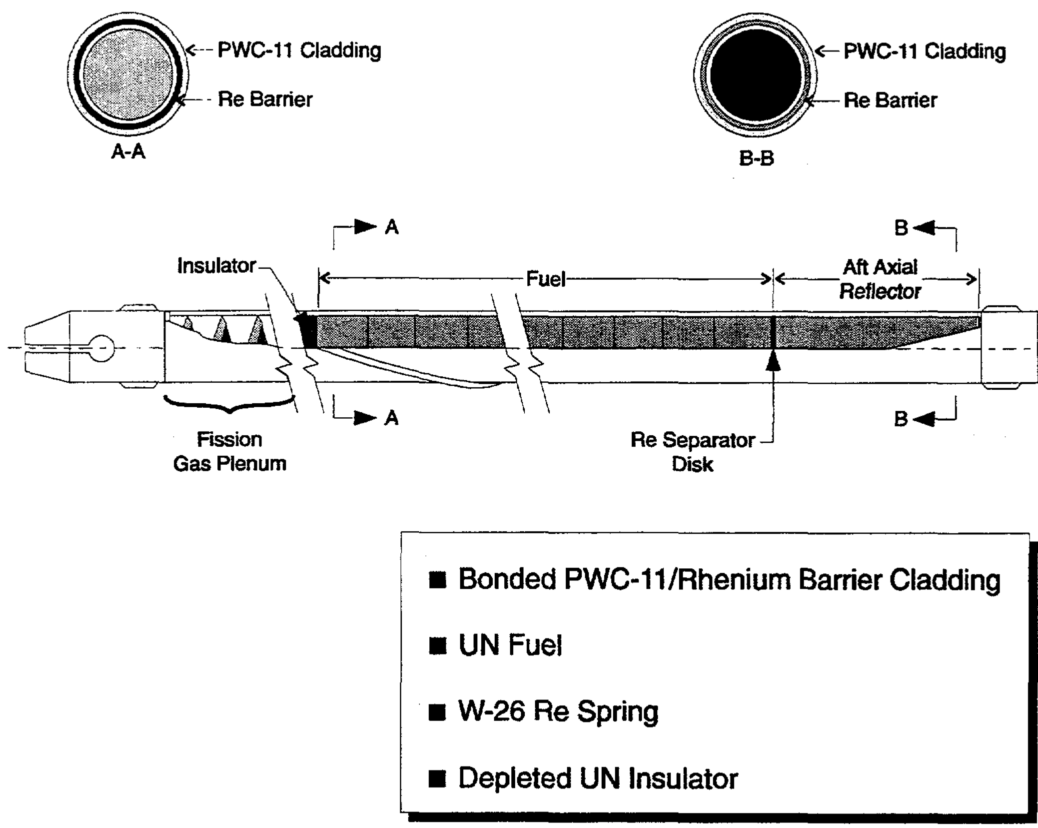

Figure 2-2. SP-100 fuel pin (Dean et al., 1991).

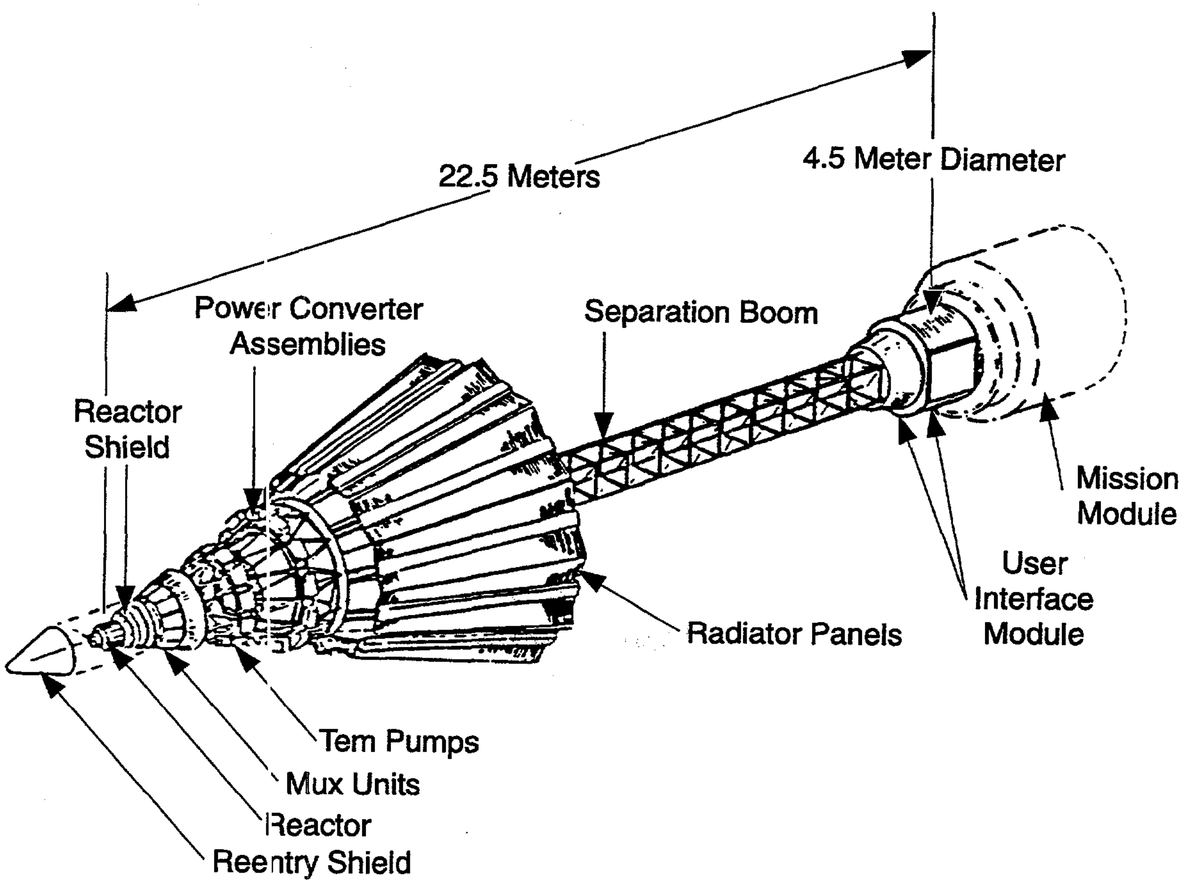

Figure 2-3. SP-100 thermoelectric space power system (GE, 1988b).

layers of beryllium, tungsten, and lithium hydride. Additional attenuation of dose is achieved by separating the payload from the reactor by a boom.

2.1.2 General Approach

Although the general approach of the RSMASS-D model for the LMR is similar to that of the RSMASS model, the treatment of the structure, pressure vessel, instrumentation, and control and safety systems has been improved. The most significant improvement is the provision for automic optimization of mass. For LMRs, important parameters for mass optimization include the pin diameter, the core length-to-diameter ratio, and fuel/cladding gap. In this model, these parameters are expressed in terms of the pin cladding outer radius (r_{oc}), the core aspect ratio (a), and the fuel smear density (*SD*).* As the pin diameter gets smaller, the allowed fuel power density increases, but the required critical mass may increase because of a reduction in the fuel volume fraction. Increasing the core aspect ratio can reduce shield size, but it will also increase the critical mass required. Decreasing the fuel smear density by increasing the gap between the fuel pellet and the rhenium liner allows greater fuel swelling without fuel damage. Hence, increased gap size can permit adequate fuel burnup with decreased fuel requirements; however, the larger gap also drives up fuel temperatures and places limits on power density. The larger gap will also decrease the fuel volume fraction and increase the required critical mass.

The method for mass optimization is to first select the pin outer radius, the core length-to-diameter, or aspect ratio, and the fuel smear density from an array of allowed design parameters. The following computation sequence (described in the remainder of Section 2.1 and in 3.2) is executed using these parameters and other fixed parameters to compute reactor and shield mass. The computation is then repeated for all allowed combinations of specified design parameters, and the reactor and shield mass are obtained for each case. The parameter choice yielding the lowest total (reactor plus shield) mass is then selected as the mass-optimized choice. When this model is incorporated in a system code, the entire system mass is calculated for all allowed combinations of design parameters to obtain the optimized total system mass.

* The smear density is defined as the fraction of theoretical density for the fuel when averaged over the area within the inside diameter of the rhenium liner.

2.1.3 Fuel Mass Calculations

2.1.3.1 Fuel Burnup

As with the RSMASS model, the fuel mass is computed first. The first step is to compute the mass of fuel burned up during reactor operation (M_B):

$$M_B = \frac{0.38Pt}{\varepsilon e}, \tag{2.1-1}$$

where P is the maximum reactor system electrical power, t is the reactor operating time, e is the net fractional efficiency, and ε is the fractional fuel enrichment.

2.1.3.2 Fuel Mass Based on Fuel Damage Considerations

Since fuel damage will limit the fraction of fuel allowed to burn up (β), a minimum fuel mass based on fuel damage limits (M_F) must be calculated. The allowed burnup fraction, however, will depend on the smear density, *SD*. From an earlier study (Marshall and McKissok, 1990), burnup fractions of about 0.06 and 0.08 are expected to be achieved for smear densities of 0.90 and 0.80, respectively. Assuming a linear relationship, we obtain

$$\beta = 0.24 - 0.2SD, \tag{2.1-2}$$

and the fuel mass based on burnup limits for fuel damage is

$$M_F = \frac{0.38Pt\,P_F}{\beta e}, \tag{2.1-3}$$

where P_F is the core spatial peak/average power factor.

2.1.3.3 Fuel Mass Based on Neutronic Considerations

The method described in Marshall (1986) is used to compute the fuel mass required based on neutronic limits (M_E). M_E is the sum of the mass of fuel burned up [M_B from Equation (2.1-1)] plus the mass of fuel needed for criticality (M_C). The original RSMASS model assumes that M_C can be estimated by using the critical mass for a fully enriched, compacted, reflected sphere of fuel material, then correcting this value for the effects of increased neutron leakage associated with the actual reactor geometry and the effects of parasitic neutron capture, lower enrichment, and other factors. Despite the inelegance of this crude assumption, the approach works surprisingly well, particularly if the critical mass can be normalized at one data point to the value of the critical mass obtained from more detailed calculations or experimental data.

Since actual reactors are not generally compacted spheres, corrections must be made for the actual geometry. It is shown in Appendix A that the correction (C_a) for a core with cylindrical geometry and an aspect ratio (core length-to-diameter ratio) of a is approximately

$$C_a = \frac{1}{3}\left(2.34a^{2/3} + a^{-4/3}\right) \qquad \text{for } (a \geq 1.0)\,. \tag{2.1-4}$$

To obtain the correction for increased leakage because of the unfueled regions in the core, the fueled fraction of the core volume, VF, must be determined. The first step in this computation is to determine the cladding thickness, t_c. For this calculation, t_c is the combined thickness of the bonded cladding and liner. Since the required cladding thickness, based on stress considerations, is directly proportional to the cladding radius, t_c can be computed using the known ratio of cladding thickness to cladding outer radius (r_{oc}) for the reference SP-100 reactor (0.129). Therefore,

$$t_c = 0.129 r_{oc}\,. \tag{2.1-5}$$

Fabrication difficulties and other limitations put a lower limit on the cladding thickness of about 5×10^{-4} m. Hence,

$$\begin{aligned} &\text{if } t_c < 5\times10^{-4} \text{ m, then set} \\ &t_c = 5\times10^{-4} \text{ m.} \end{aligned}$$

The cladding inner radius, r_{ic}, is then

$$r_{ic} = r_{oc} - t_c\,. \tag{2.1-6}$$

Assuming a solid fuel pellet fraction with a theoretical density of 0.96, and defining

$$C_s = \sqrt{\frac{SD}{0.96}}\,, \tag{2.1-7}$$

the fuel pellet radius, r_f, is

$$r_f = C_s r_{ic}\,. \tag{2.1-8}$$

For pins on a hexagonal pitch, the unit cell fuel area, A_f, and the total cell hexagonal area, A_h, are given by

$$A_f = 3\pi r_f^2 \tag{2.1-9}$$

and

$$A_h = 2.6\left(2r_{oc} + 5\times10^{-4}\right)^2, \tag{2.1-10}$$

respectively. It is assumed here that the wire wrap thickness between fuel pins is fixed at 5×10^{-4} m. Assuming 20 percent of the core volume is required for in-core safety rods and 10 percent of the core volume is needed for auxiliary cooling system thimbles, the volume fraction of fuel in the core can now be computed as

$$VF = 0.7\frac{A_f}{A_h}. \tag{2.1-11}$$

Marshall (1986) shows that the correction for the fuel volume fraction is approximately

$$\left(\frac{13{,}600}{VF\rho_F}\right)^{1.5},$$

where ρ_F is the unhomogenized fuel density and 13,600 designates the fuel density used in the critical mass calculation for a compacted, reflected sphere of 93 percent enriched UC_2.

Since these computations are restricted to LMRs of the SP-100 type, smaller corrections are required if the core average fuel density for the reference SP-100 reactor is used (5431 kg/m^3) rather than the full fuel density of 13,600 kg/m^3 used in RSMASS. The correction for fuel volume fraction and density becomes

$$\left(\frac{5431}{VF\rho_F}\right)^{1.5}.$$

When the core average fuel density is used, the reference critical mass, M_{CR}, is the value for the actual reference core, rather than for a compacted sphere. The value of M_{CR} was chosen to match the resulting end-of-life critical mass with the critical mass obtained from detailed calculations for the reference reactor (see LMR input parameters in Table B-1).

Another total correction factor, C, can be used to account for other (miscellaneous) effects on the critical mass, and we define

$$C = C_a C_m, \tag{2.1-12}$$

which is a combined correction factor for the aspect ratio and miscellaneous effects. Although corrections for parasitic capture in the rhenium in the core could be included in the C correction, these effects have been included in the reference critical mass provided in the recommended input parameters in this document (Table B-1).

The calculational scheme in Marshall (1986) also accounts for the effect of enrichment on critical mass. The $1/\varepsilon^2$ correction derived in Marshall (1986) works well for fast reactors and will be included in the mass correction. In general, however, it is best to simply assume a fully enriched reactor ($\varepsilon = 0.93$), since we are only interested in the minimum critical mass. Our final equation for the initial critical mass, M_C^0, is then given by

$$M_C^0 = \frac{CM_{CR}}{\varepsilon^2}\left(\frac{5431}{VF\rho_F}\right)^{1.5}. \tag{2.1-13}$$

From Marshall (1986), the end-of-life critical mass, M_C, is approximately

$$M_C = \frac{M_C^0 + \sqrt{\left(M_C^0\right)^2 + 4M_C^0 M_B (1-\varepsilon)}}{2}, \tag{2.1-14}$$

and the end-of-life total fuel mass required based on neutronic limits, M_E, is

$$M_E = M_C + M_B. \tag{2.1-15}$$

2.1.3.4 Fuel Mass Based on Thermal Considerations

Fuel mass requirements may also be determined by thermal considerations and temperature limitations on materials. We can compute this fuel mass limitation by first computing the specific power limit, P_s, which is the maximum thermal power that can be obtained per kilogram of fuel without exceeding material temperature limits. In this document the thermal analysis will use volume-adjusted thermal resistances (R^T) to simplify the computation of specific power; i.e., the equations for thermal resistances have been multiplied by the expression for fuel volume.

The specific power is calculated based on pin dimensions, fuel temperature limits, T_f, and the coolant temperature, T_c. The overall volume-adjusted thermal resistance, R_T^T, is dominated by the fuel/cladding gap volume-adjusted thermal resistance, R_g^T, which depends on the gap conductance. Assuming that the gap conductance is dominated by conductivity through the helium fill gas, an effective gap conductivity, k_g, can be expressed as

$$k_g = \frac{k}{r_f \ln\left(\frac{r_{ic}}{r_f}\right)} \tag{2.1-16}$$

The conductivity of the helium fill gas, k, has been adjusted slightly in the recommended input parameters (Table B-1) to obtain better agreement with more detailed calculations.

The volume-adjusted thermal resistances across the fuel pin are then computed:

$$R_f^T = r_f^2 / 4k_f, \tag{2.1-17}$$

$$R_g^T = r_f / 2k_g, \tag{2.1-18}$$

$$R_{Lc}^T = \frac{r_f^2 \ln(r_{oc}/r_{ic})}{2k_{Lc}}, \tag{2.1-19}$$

$$R_c^T = r_f^2 / 2r_{oc}h_c, \tag{2.1-20}$$

and

$$R_T^T = R_f^T + R_g^T + R_{Lc}^T + R_c^T. \tag{2.1-21}$$

R_f^T, R_g^T, R_{Lc}^T, and R_c^T are the volume-adjusted thermal resistances for the fuel pellet, gap, liner cladding, and coolant, respectively, and R_T^T is the total volume-adjusted thermal resistance. The variables k_f and k_{Lc} are the thermal conductivities for the fuel and liner cladding, respectively; h_c is the heat transfer coefficient for the coolant.

The maximum allowed specific power is computed next:

$$P_s = \frac{T_f - T_c}{\rho_F R_T^T \times 10^6}, \tag{2.1-22}$$

where T_f and T_c are the maximum fuel temperature and the core outlet bulk coolant temperature, respectively. Finally, the fuel mass based on thermal limits, M_p, is

$$M_p = \frac{PP_F}{P_s e}. \tag{2.1-23}$$

2.1.4 Limiting Fuel Mass

The actual required fuel mass, M_L, will be the largest of the fuel mass requirements based on neutronic, thermal, and fuel damage limits, or

$$M_L = \text{greatest of } M_E,\, M_p, \text{ and } M_F. \tag{2.1-24}$$

2.1.5 Reactor Component Mass Calculations

2.1.5.1 Structural Mass Calculation

To compute the structural mass, the core structure is divided into fuel pin hardware (e.g., end fittings), miscellaneous structure (reflector support, honeycomb structure, and insulation), and bonded cladding/liner structure. The fuel pin hardware structure and miscellaneous structure are assumed to scale roughly with core volume. From data for the reference SP-100 reactor, a core average structural density of 1183 kg/m^3 was obtained for the miscellaneous structure. The structural density for fuel pin hardware was determined to be approximately equal to the miscellaneous structural density. The cladding and liner structural mass, however, will depend on both the core volume and the required length of the fission gas plenum, which depends on the quantity of fission gas generated. The method for treating the cladding structure follows.

We first compute the total core volume, V,

$$V = \frac{M_L}{VF\rho_F}. \tag{2.1-25}$$

The core diameter, D, and core length, L, are then

$$D = \left(\frac{4V}{a\pi}\right)^{1/3} \tag{2.1-26}$$

and

$$L = aD. \tag{2.1-27}$$

burnup fraction limits, M_F. If the fuel mass for a particular selection of parameters is not determined by burnup fraction (fuel damage) limitations, the fission gas generated per kilogram of fuel will be less than for the reference case, and a smaller plenum will be sufficient. In other words, if $M_F < M_L$, the reduction in fission gas volume required relative to the reference plenum volume will be reduced by the factor M_F / M_L. This ratio is obtained by noting that the required fission gas volume, for design gas pressure in the pins, is proportional to M_F for the case being calculated and is proportional to M_L for the reference case.

Because the required plenum volume is proportional to the fission gas volume and length, i.e.,

$$L_p = L\left(\frac{M_F}{M_L}\right), \qquad (2.1\text{-}28)$$

it follows that L_p = the core length, L, when $M_F = M_L$, as for the reference case. Since M_F cannot exceed M_L, L_p/L is always less than or equal to 1.0. It is assumed that a minimum plenum length of 0.06 m will always be required; consequently,

if $L_p < 0.06$ m, then set

$$L_p = 0.06 \text{ m}.$$

Obtaining a good approximation for L_p is also necessary for the calculation of pressure vessel and shielding mass (see Sections 2.1.5.3 and 3.2.1).

From the reference SP-100 reactor data, we can then estimate the total structural mass, M_s, by

$$M_s = V\left[2366 + 2320\left(\frac{L_p + L}{2L}\right)\right]. \qquad (2.1\text{-}29)$$

The value of 2366 is the approximate core average structural density for the miscellaneous structure (1183 kg/m^3) plus the approximately equal core average density for the fuel pin hardware. The value of 2320 kg/m^3 is the approximate core average cladding density (including the plenum region).

2.1.5.2 Reflector Mass Calculation

No axial reflectors are assumed for the LMR model; hence, the reflector is represented by an annulus of volume

$$\pi\left[\left(\frac{D}{2}+T\right)^2-\left(\frac{D}{2}\right)^2\right](L+T), \tag{2.1-a}$$

where D is the core diameter and T is the reflector thickness. Hence, the total reflector mass, M_{Rf}, is

$$M_{Rf}=\rho_{Rf}\pi(T^2+DT)(L+T), \tag{2.1-30}$$

where ρ_{Rf} is the reflector density.

2.1.5.3 Pressure Vessel Calculation

The pressure vessel radius, r_{pv}, and length, L_{pv}, are given by

$$r_{pv}=F_{rp}\left(\frac{D}{2}+nT\right) \tag{2.1-31}$$

and

$$L_{pv}=F_{Lp}\ (L+L_p). \tag{2.1-32}$$

F_{rp} and F_{Lp} are multipliers on the core radius and total pin length, respectively, obtained from design data. The parameter n is the pressure vessel locator. A value of zero is recommended for n, since using zero locates the pressure vessel inside the reflectors. As an option, n can be set to 1, which places the pressure vessel outside the reflectors.

As described in Marshall (1986), the pressure vessel thickness, t_{pv}, assuming a safety factor of 4.0, is approximately

$$t_{pv}=\frac{3P_r r_{pv}}{U_s}, \tag{2.1-33}$$

where P_r is the reactor coolant pressure, and U_s is the ultimate strength of the pressure vessel material.

A minimum pressure vessel thickness of t_{min} is specified (Table B-1), such that

$$\text{if } t_{pv} < t_{\min}, \text{ then}$$

$$t_{pv} = t_{\min}.$$

Finally, the pressure vessel mass, M_{pv}, is estimated by

$$M_{pv} = 6\pi r_{pv}\rho_{pv}t_{pv}\,(r_{pv} + L_{pv}), \tag{2.1-34}$$

where ρ_{pv} is the pressure vessel density. Equation (2.1-34) roughly accounts for the SP-100 pressure vessel geometry, and experience has shown that M_{pv} should be multiplied by a factor of 3.0 to account for additional pressure vessel structure, flanges, etc. Although this estimate is crude, the contribution of the pressure vessel to the total reactor mass is relatively small and has only a minor impact.

2.1.5.4 Coolant Mass Calculation

The lithium coolant mass in the reactor, M_{Lc}, is roughly proportional to the core volume. From reference SP-100 data, the reactor coolant mass is approximated by

$$M_{Lc} = 916V. \tag{2.1-35}$$

2.1.6 Total Reactor Mass

The total reactor mass, M_R, is the sum of the fuel mass and the reactor-component masses:

$$M_R = M_L + M_s + M_{Rf} + M_{pv} + M_{Lc}. \tag{2.1-36}$$

2.1.7 Mass Calculations for Ancillary Systems

Instrumentation and control (I&C) mass and safety system mass were included as part of the total reactor mass in Marshall (1986). For RSMASS-D models, these are separate from the total reactor mass. The methods for calculating I&C mass and safety mass are described below.

2.1.7.1 Instrumentation and Control Mass Calculation

Instrumentation and control mass is assumed to be composed of three components: a fixed component, a size-dependent component, and a boom-length-dependent component. (Boom mass calculations for LMR systems are explained in Section 3.2.3.) The fixed component includes such items as the controller, multiplexers, sensors, and local cables, which are items that should not change appreciably with reactor size or power level. The size-dependent I&C

component includes actuators, drives, and launch support I&C. Size-dependent hardware is assumed to be proportional to the effective core area, A, defined as

$$A = \left(\frac{2V}{\pi}\right)^{2/3}. \tag{2.1-37}$$

The boom-length-dependent component consists of the I&C cables running the length of the payload separation boom. Hence, the I&C mass (M_{IC}) is approximated by

$$M_{IC} = d_1 + d_2 A + d_3 Rp, \tag{2.1-38}$$

where d_1 is the mass of the fixed I&C component, d_2 is the areal density of the size-dependent I&C, d_3 is the mass/length of the I&C cables, and R_p is the separation distance between the reactor and payload. The values for d_1, d_2, and d_3 have been determined from data for the reference SP-100 system and are given in the recommended LMR parameters in this document (Table B-1).

2.1.7.2 Safety System Mass Calculation

The safety systems for LMRs are assumed to include in-core safety rods, an auxiliary core cooling system (ACS), a rhenium barrier surrounding the core to ensure water-flooded subcriticality, and a reentry heat shield. The safety rod system and miscellaneous safety components (ACS and rhenium barrier) are assumed to be proportional to an effective core radius, r_{eff}. For example, the rhenium barrier surrounds the core circumference and is therefore proportional to the core radius. The effective core radius is defined as

$$r_{\text{eff}} = \left(\frac{3V}{4\pi}\right)^{1/3}. \tag{2.1-39}$$

From the reference SP-100 data, the following is obtained:

$$M_{MS} = 248 r_{\text{eff}} \tag{2.1-40}$$

and

$$M_{SR} = 389 r_{\text{eff}}, \tag{2.1-41}$$

where M_{MS} is the miscellaneous safety system mass, and M_{SR} is the mass of the safety rod system.

The reentry heat shield consists of a nose cone and a truncated conical section that surrounds the reactor. The nose cone mass, M_{NC}, is approximated by

$$M_{NC} + 1.6\,(222 r_{pv}^2 - 1.75 r_{pv})\,. \tag{2.1-42}$$

[The constants in Equations (2.1-43) through (2.1-48) were obtained from data for the reference SP-100 reactor system.]

For the truncated conical section, the radii of the cone are first computed:

$$R_a = r_{pv} + 0.0177\,, \tag{2.1-43}$$

$$R_b = R_a + 0.0059, \tag{2.1-44}$$

$$\theta = \tan^{-1}\left[\frac{D_{pay}/2 - (r_{pv} + T)}{L_{pv} - 0.21 + R_p}\right], \tag{2.1-45}$$

$$R_c = r_{pv} + L(\tan\theta), \tag{2.1-46}$$

and

$$R_d = R_c + 0.0059. \tag{2.1-47}$$

R_a and R_b are the inner and outer radii at the narrow end of the conical shield, and R_c and R_d are the inner and outer radii at the wide end of the conical shield. R_p is the payload separation distance from the core, D_{pay} is the payload diameter, and θ is the radiation shield cone half angle. The mass of the conical shield (M_{CS}) is given by

$$M_{CS} = 1600(L_{pv} - r_{pv})\,[(R_b^2 + R_b R_d + R_d^2) - (R_a^2 + R_a R_c + R_c^2)]\,, \tag{2.1-48}$$

and the total heat shield mass, M_{HS}, is

$$M_{HS} = M_{NC} + M_{CS}. \tag{2.1-49}$$

The total safety system mass, M_{SS}, is

$$M_{SS} = M_{MS} + M_{SR} + M_{HS}. \tag{2.1-50}$$

2.2 In-Core Thermionic Reactors

2.2.1 Reactor Description

The thermionic fuel element reactor concept is at present the most developed in-core thermionic reactor approach; consequently, the basic TFE design will be assumed for the in-core thermionic reactor model. TFE reactor cores may consist of exclusively TFE fuel elements (all-TFE fuel elements), a mixture of TFE and SNAP (system for nuclear auxiliary power) driver fuel elements, or TFE fuel elements with a moderator (TOPAZ). In the RSMASS-D mass optimization scheme, the reactor and shield mass for all of the model options are computed and the option and parameter choice yielding the lowest mass is selected as the mass-optimized choice. These options are discussed in GA (1989, 1987b), and SPI (1987a). A description of these various options follows.

The TFE-based reactor concept employs cylindrical fuel elements that are stacked on end in a manner analogous to dry cells in a flashlight (Figure 2-4). The converter stack is encased in a metallic cladding to form a thermionic fuel element. Each cell consists of an arrangement of annular uranium dioxide fuel pellets surrounded by a tungsten emitter, a cesium vapor-filled gap, a collector, and an insulator sheath (Figure 2-5). During power operation, heat from the nuclear fuel boils electrons off of the hot (~1880 K) emitter surface. These electrons cross the interelectrode gap to the cooler (~1000 K) collector surface. The voltage potential between the emitter and collector is used to drive the current through the electrical load. All three concepts use a sodium/potassium (NaK) coolant and incorporate rotating reflector/control drums within the pressure vessel surrounding the core. Radiation shields for these concepts are assumed to use layers of zirconium hydride and lithium hydride.

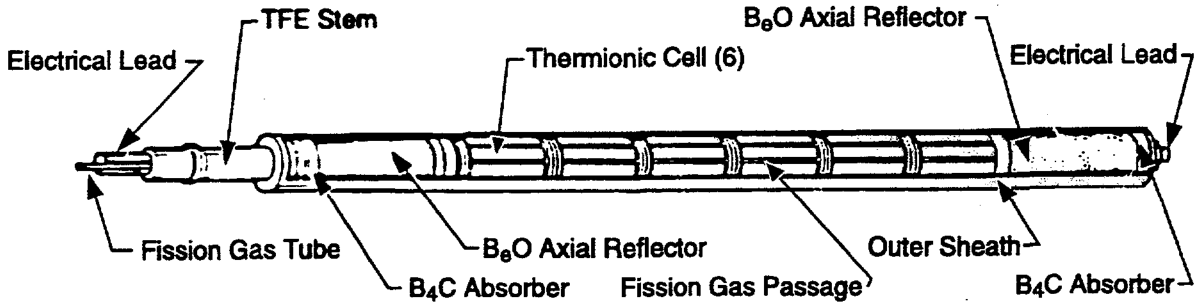

Figure 2-4. Thermionic fuel element (GA, 1985).

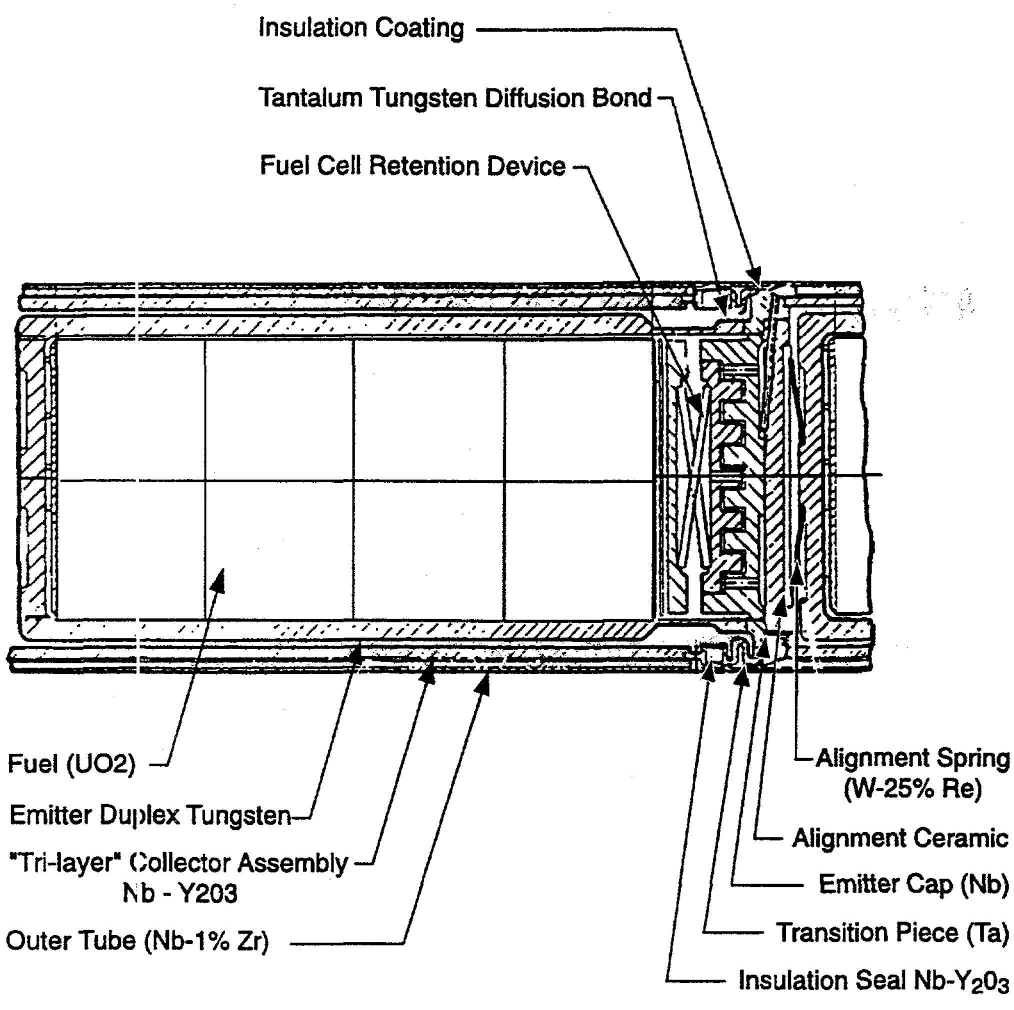

Figure 2-5. Thermionic fuel cell (GA, 1985).

The all-TFE concept (Figure 2-6) is a fast reactor with no moderator or driver fuel. The absence of a moderator or driver fuel permits coolant temperatures up to 1000 K or more. The all-TFE concept is most suitable for higher power levels (≥ 100 kWe).

The Russian TOPAZ reactor designs (Figure 2-7) incorporate a zirconium hydride moderator between the fuel elements to reduce critical mass requirements. The presence of a zirconium hydride moderator limits coolant temperatures to about 900 K. Because the thermal neutron cross section for natural tungsten is too high to permit its use in a moderated reactor, tungsten-184 would have to be used for emitter fabrication. Two TOPAZ reactor systems have been developed by the Russians. TOPAZ I incorporates stacked fuel elements and is referred to as the multicell approach. Except for the use of a moderator, the thermionic fuel element design assumed for the TOPAZ I concept is identical to the thermionic fuel element concept illustrated in Figures 2-4 and 2-5. The other TOPAZ design is referred to as TOPAZ II. TOPAZ II uses a single-cell design, rather than a stack of multicells. No parameter changes have been implemented to reflect the small structural mass differences between TOPAZ I and TOPAZ II.

In the driver fuel concept (Figure 2-8), auxiliary nonthermionic fuel elements are used to make up some of the required critical mass. The concept uses SNAP reactor-type fuel elements [zirconium hydride with 15 weight percent (wt%) uranium loading] as the driver fuel elements. Nuclear heat produced in the driver fuel is not utilized for electrical power; consequently, this approach is not as efficient as the other two thermionic fuel element concepts. The use of SNAP fuel also limits coolant temperatures to about 900 K.

2.2.2 General Approach

The TFE model was more difficult to develop and is more complex than the LMR or OTR concepts since all three basic types of TFE reactors must be considered. The model must also explore various thicknesses of moderator and various loadings of driver fuel (including no moderator and no driver fuel).

The problem is further complicated by the heterogeneous effects of a moderated geometry that depends on the thickness of the moderator and other considerations. Furthermore, when driver fuel is present, some of the power is produced in the driver fuel as well as the TFE, and the relative amount depends on the driver fuel loading and the degree of flux tilting in the moderator region.

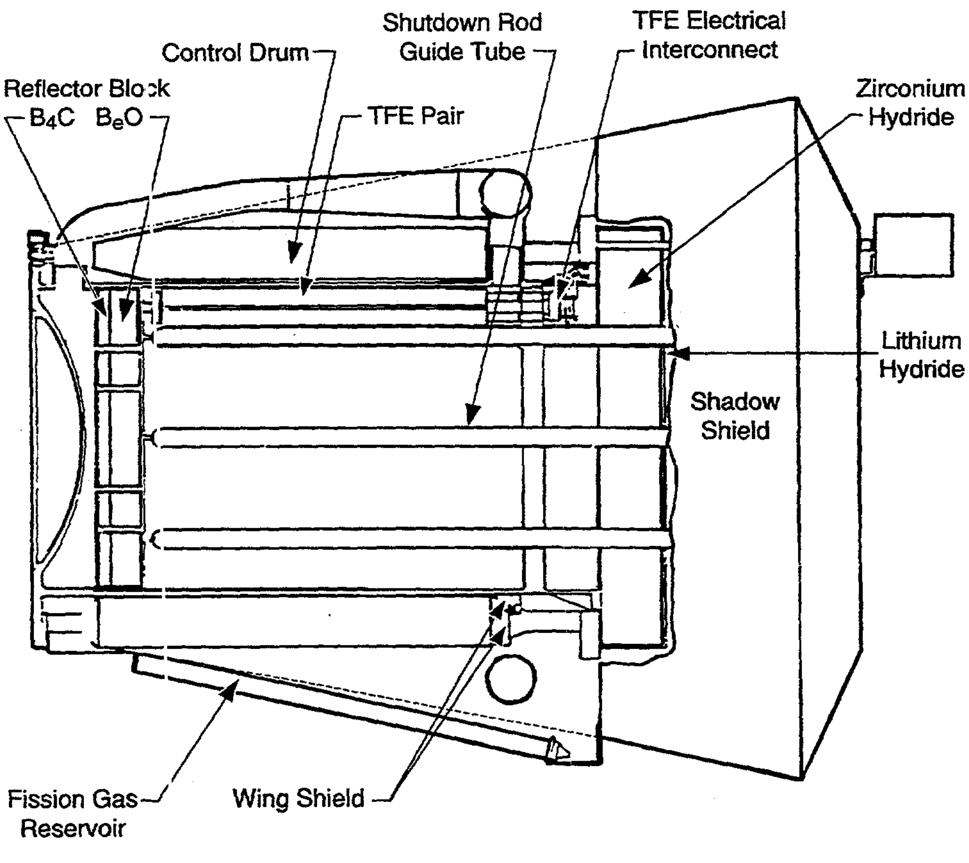

Figure 2-6. All-TFE space reactor (GA, 1985).

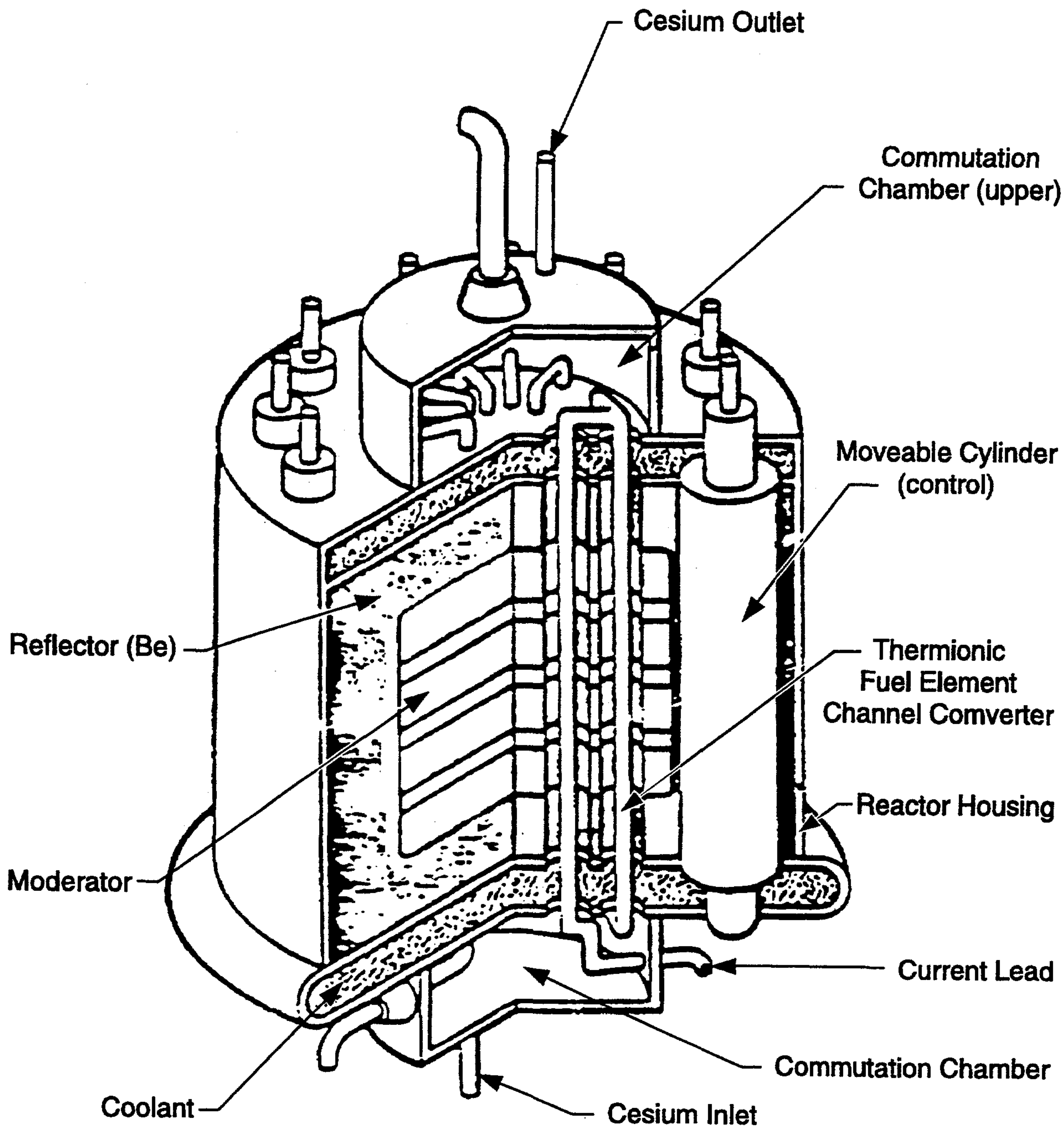

Figure 2-7. TOPAZ-moderated TFE space reactor (Sholtis et al., 1994).

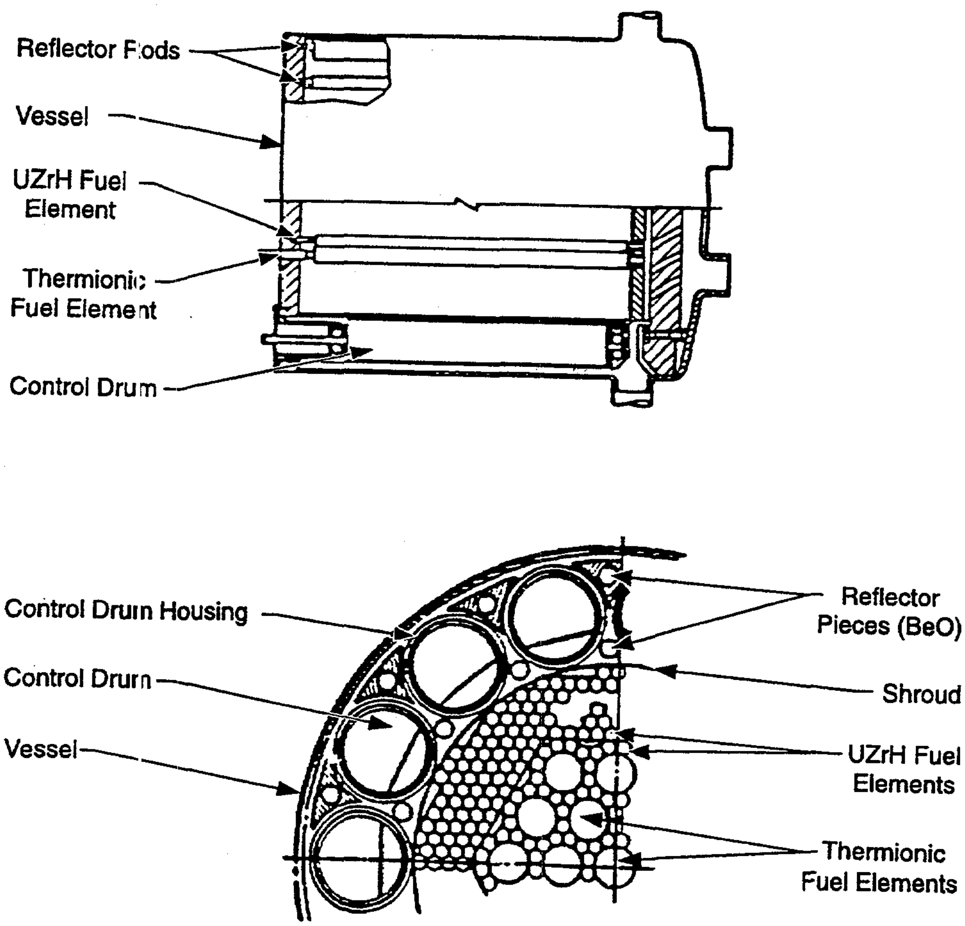

Figure 2-8. Moderated TFE reactor with driver fuel (GA, 1987b).

Reactor mass is minimized by varying the emitter radius, r_e, the uranium loading in the driver fuel, U_{LD}, the moderator thickness, T_m, and the reactor core aspect ratio, a. (In the system program that uses RSMASS-D the emitter/collector temperature is also varied.) The emitter radius will affect the fuel volume fraction and the relative loading of TFE fuel to driver fuel, which will both affect critical mass. The emitter radius will also affect the maximum allowed specific power, as well as the available relative emitter surface area. The choice of driver fuel loading reflects a trade-off between critical mass considerations and net efficiency. Moderator thickness affects critical mass, flux tilting, power distribution, overall core size, and other considerations. The principal trade-off for the aspect ratio is the critical mass and the shield mass.

The reference critical mass for the TFE reactor concept is not a single value, as in the case of the LMR model. It depends on the driver fuel uranium loading, U_{LD}, the thickness of the moderator region, T_m, and the emitter radius, r_e. As for the LMR model, values for variable parameters are selected and the computational sequence described in the remainder of Section 2.2 and in Section 3.3 is executed to compute the reactor and shield masses, respectively. The computation is then repeated for all allowed combinations of design parameters to obtain the reactor and shield mass for each case. The parameter combination yielding the lowest reactor plus shield mass is then selected as the mass-optimized design.

2.2.3 Fuel Mass Calculations

2.2.3.1 Fuel Mass Based on Neutronic Considerations

The variable parameters selected at this point are the uranium loading, the emitter radius, the moderator thickness, and the core aspect ratio.

First, the driver region fuel density, ρ_{fD}, is computed. For a selected driver region uranium load (U_{LD}, in wt%), fuel density is given by

$$\rho_{fD} = 615 U_{LD}. \quad (2.2\text{-}1)$$

Based on design data for large (Merril, 1986) and small (SPI, 1987b) TFE cells, we can use a linear fit to approximate the volume fraction of fuel in the TFE pin (VF_p) and the TFE unit cell (VF_c) as follows:

$$VF_p = 5.75 r_e + 0.327 \quad (2.2\text{-}2)$$

and

$$VF_c = 10.92r_e + 0.207, \qquad (\text{for } r_e < 0.02 \text{ m}) \tag{2.2-3}$$

where r_e is the emitter radius (see Figure 2-9). Based on stress considerations and representative design data, the TFE fuel pellet, pin, and TFE effective cell radii (r_f, r_p, and r_t respectively) are assumed to scale as

$$r_f = 0.881 r_e, \tag{2.2-4}$$

$$r_p = 1.332 r_f, \tag{2.2-5}$$

and

$$r_t = r_p \sqrt{\frac{VF_p}{VF_C}}. \tag{2.2-6}$$

Using a cylindrical cell geometry and surrounding the TFE cell with an annulus of moderator (with or without driver fuel in the moderator zone), the driver/moderator outer radius, r_D, is

$$r_D = r_t + T_m, \tag{2.2-7}$$

where T_m is the thickness of the moderator region.

Assuming that 20 percent of the driver/moderator region is either void or consists of some material other than fuel or moderator, the total unit cell radius (r_c) becomes

$$r_c = \sqrt{1.2r_D^2 - 0.2r_t^2}. \tag{2.2-8}$$

If no driver fuel is assumed ($U_{LD} = 0.0$), the critical mass of uranium is associated entirely with the fuel in the TFE fuel elements. The critical mass of the TFE fuel (M_{cT}^c) was obtained by first computing flux-weighted cell-averaged cross sections, using the finite-element multigroup P_n (FEMP) transport theory code (McDaniel and Harris, 1983) in cylindrical geometry (Figure 2-10). These calculations were carried out for several emitter radii and several thicknesses of moderator region. The flux-weighted cross sections were then used in FEMP transport theory calculations assuming the geometry illustrated in Figure 2-11. The core region was modeled as a sphere surrounded by a 10.0 cm BeO reflector. Using appropriate flux-weighted cross sections and atom densities, a series of transport theory calculations were

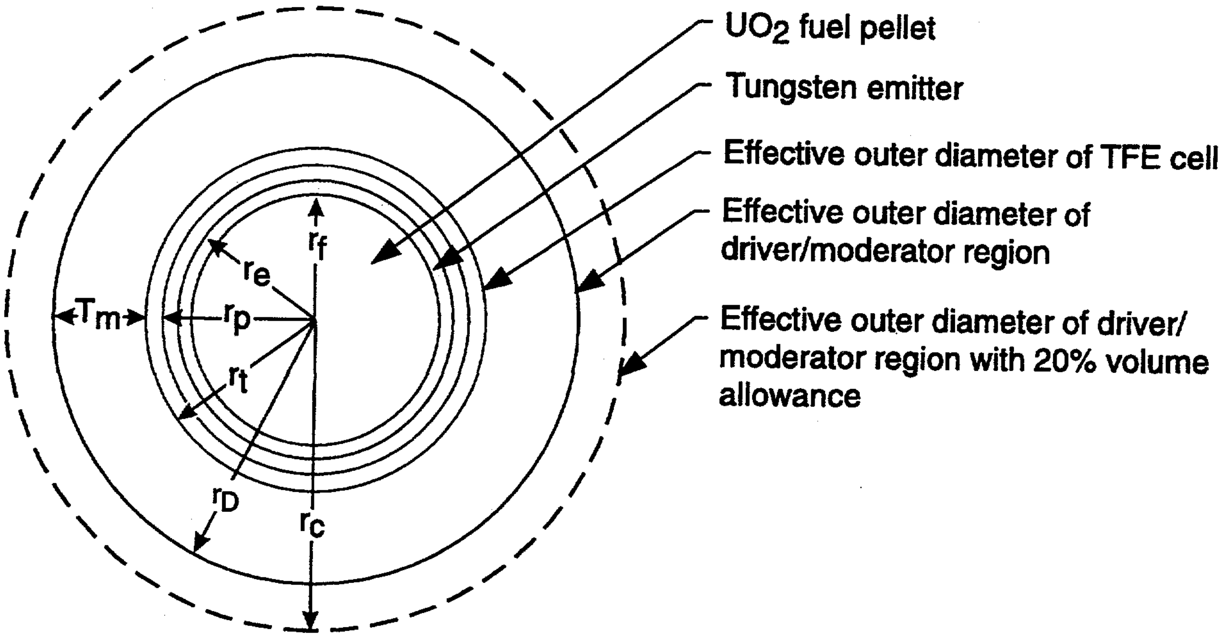

Figure 2-9. Assumed TFE cell geometry.

performed to determine the required critical mass, M_{cT}^{c}, for various emitter radii and moderator region thicknesses. The results of these calculations have been plotted as a function of T_m and r_e and are tabulated in Table 2-1. Hence, for the selected values of T_m and r_e, the TFE critical mass, M_{cT}^{c}, is obtained from the M_{cT}^{c} matrix in Table 2-1. The driver fuel component of the critical mass, M_{cD}^{c}, is zero for these cases.

For $U_{LD} > 0.0$, the transport theory results were also plotted for M_{cD}^{c} as a function of U_{LD} and r_e and are tabulated in Table 2-2. Here U_{LD} is defined as the weight percent of uranium-235 in the $ZrH_{1.7}$ matrix. Although the total critical mass ($M_{cT}^{c} + M_{cD}^{c}$) is a strong function of the driver/moderator region thickness, the driver fuel component is found to be only a weak function of T_m; consequently, the two-dimensional matrix given in Table 2-2 is adequate for determining M_{cD}^{c}. Loadings less than 3.5 wt% are probably impractical, and using a 3.5 wt%

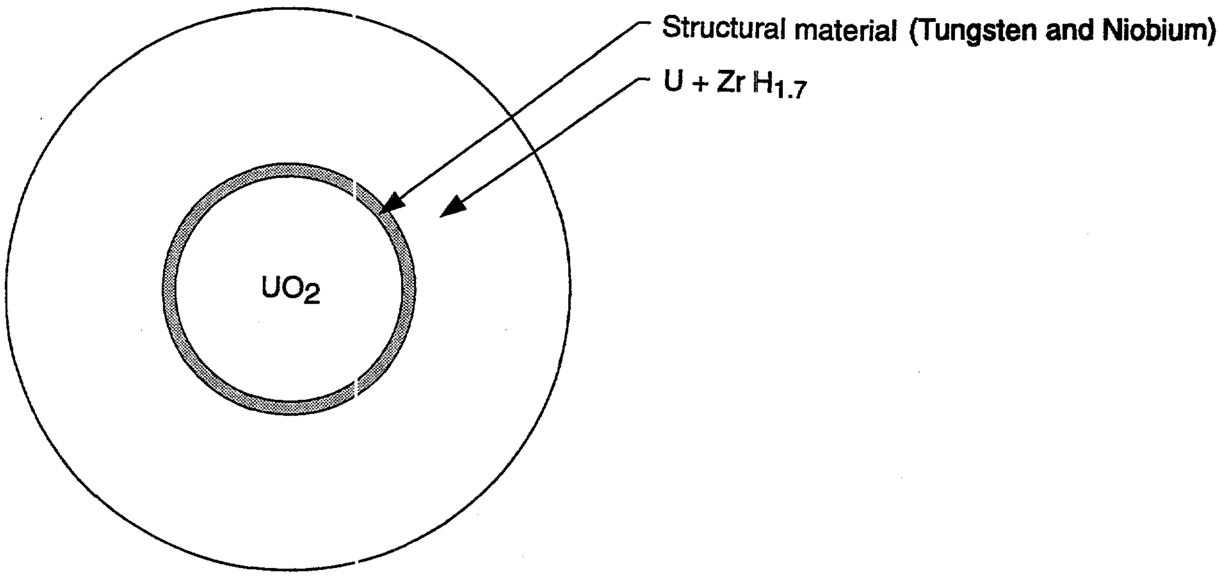

Figure 2-10. Cylindrical cell geometry used to obtain flux-weighted cross sections for TFE cells.

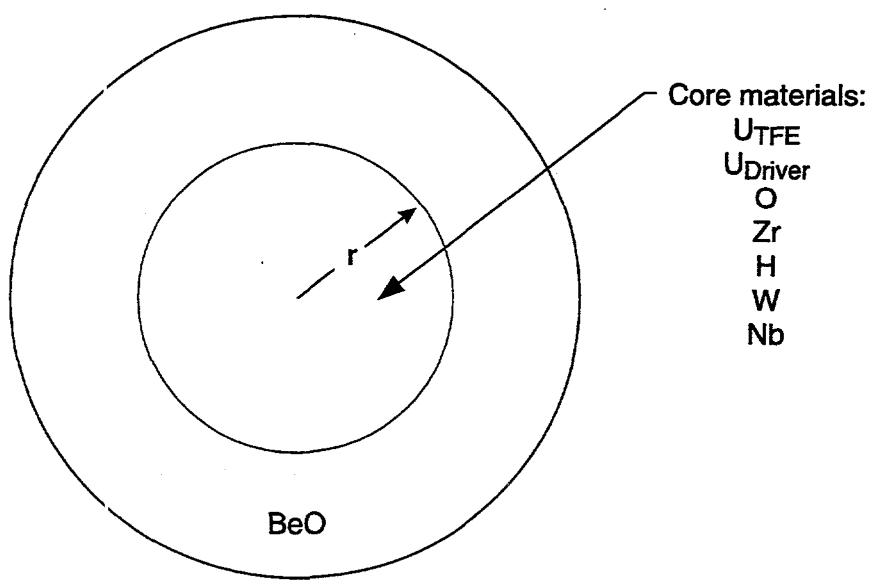

Figure 2-11. Compacted sphere geometry used to obtain critical mass data for TFE reactors.

Table 2-1. Critical Mass for TFE Fuel [M_{cT}^{c} (kg)] with No Driver Fuel Used

	r_e (m)			
T_m (m)	0.00568	0.0075	0.01005	0.0144
0.0	101.0	88.0	79.2	65.9
0.0035	45.0	41.0	39.0	42.0
0.0070	22.5	23.0	23.2	26.5
0.0120	30.0	24.0	22.0	21.0
0.144	216.4	41.0	21.3	19.8

Table 2-2. Critical Mass for Driver Fuel $\left[M_{cD}^{c}(kg)\right]$

	r_e (m)		
U_{LD}(wt%)	0.00568	0.01005	0.0144
3.5	2.4	2.0	1.9
8.5	4.9	4.6	4.0
17.0	8.3	7.9	6.9

minimum simplifies the algorithm. Hence, loadings less than 3.5 wt%, but not zero, are not permitted. The TFE component of the critical mass, M_{cT}^{c}, can then be obtained from the following equation:

$$M_{cT}^{c} = \frac{r_t^2 VF_c M_{cD}^{c} \rho_{fT}}{(r_c^2 - r_t^2)\rho_{fD}}, \qquad (2.2\text{-}9)$$

$$\left[\text{Can also be expressed as } M_{cT}^{c} = \frac{0.833 r_t^2 VF_c M_{cD}^{c} P_{ft}}{(R_D^2 - r_t^2) P_{fD}}\right]$$

where ρ_{fT} is the density of the TFE UO_2 fuel pellets.

Since some of the thermal power will be produced in the driver fuel region, the power division between the TFE and driver fuel region must be determined. The ratio of the power density in the driver fuel region to the power density in the TFE region, P_{SR}, was computed for several T_m from the cylindrical cell calculations that were used to obtain the flux-weighted cross sections. The results of this computation are presented in Table 2-3.

Table 2-3. Ratio of Power Density of Driver Region to TFE Region

T_m (m)	P_{SR}
0.0	1.0
0.0035	2.3
0.0070	3.0
0.0140	4.35

Next, the required thermal power in the TFE fuel, P_T, is computed:

$$P_T = \frac{P}{e_T} \qquad (2.2\text{-}10)$$

where P is the maximum reactor electrical power, and e_T is the thermionic efficiency. It can be shown that the thermal power in the driver fuel region, P_D, is given by

$$P_D = \frac{P_{SR} P_T M^c_{cD}}{M^c_{cT}}, \qquad (2.2\text{-}11)$$

where P_{SR} is obtained from Table 2-3 for the selected value of T_m. The total reactor fractional efficiency (e_R) is then

$$e_R = \frac{P}{P_T + P_D}. \qquad (2.2\text{-}12)$$

Now the quantity of uranium burned up in the TFE region, M_{BT}, and in the driver fuel region, M_{BD}, can be computed:

$$M_{BT} = \frac{0.38 P_T t}{\varepsilon} \qquad (2.2\text{-}13)$$

and

$$M_{BD} = \frac{0.38 P_D t}{\varepsilon}, \qquad (2.2\text{-}14)$$

where t is the full-power operating time.

As with the LMR model, the impact of the core aspect ratio on critical mass is computed as a correction factor

$$C_a = \frac{1}{3}(2.34a^{2/3} + a^{-4/3}) \qquad \text{for } a \geq 1.0\,, \tag{2.2-15}$$

and the total critical mass correction factor is given by

$$C = C_a C_m. \tag{2.2-16}$$

If in-core safety rods or cooling loops are required, the volume fraction of fuel and moderator in the reactor will be reduced, resulting in a net increase in the critical mass. Using the approach given in Marshall (1986), we can estimate the initial required critical mass for the TFE and driver fuel regions (M_{cT}^0 and M_{cD}^0, respectively) with a void fraction for safety hardware in the core, VF_{SH}, by

$$M_{cT}^0 = CM_{cT}^c\left(\frac{1}{1-VF_{SH}}\right)^{1.5} \tag{2.2-17}$$

and

$$M_{cD}^0 = CM_{cD}^c\left(\frac{1}{1-VF_{SH}}\right)^{1.5}. \tag{2.2-18}$$

Then the end-of-life critical mass for the TFE and driver fuel (M_{cT} and M_{cD}, respectively) can be calculated:

$$M_{cT} = \frac{M_{cT}^0 + \sqrt{(M_{cT}^0)^2 + 4M_{cT}^0 M_{BT}(1-\varepsilon)}}{2} \tag{2.2-19}$$

and

$$M_{cD} = \frac{M_{cD}^0 + \sqrt{(M_{cD}^0)^2 + 4M_{cD}^0 M_{BD}(1-\varepsilon)}}{2}. \tag{2.2-20}$$

The total end-of-life fuel mass based on criticality and fuel burnup is then,

$$M_{ET} = M_{cT} + M_{BT} \tag{2.2-21}$$

and

$$M_{ED} = M_{cD} + M_{BD} \tag{2.2-22}$$

where M_{ET} and M_{ED} are the required end-of-life fuel mass based on neutronics for the TFE and driver regions, respectively. The total end-of-life fuel mass based on neutronics, M_E, is then

$$M_E = M_{ET} + M_{ED} \tag{2.2-23}$$

Once U_{LD}, T_m, and r_e have been selected, the ratio of driver fuel to TFE fuel (R_m) is fixed; having computed M_{ED} and M_{ET}, R_m can be obtained:

$$R_m = \frac{M_{ED}}{M_{ET}}. \tag{2.2-24}$$

R_m will be used in the following subsections.

2.2.3.2 Fuel Mass Based on Fuel Damage Considerations

The amount of fuel required based on fuel damage limits (M_{FT} and M_{FD} for the TFE and driver fuel, respectively) will depend on the burnup limits for the TFE fuel, β_T, and drive fuel, β_D:

$$M_{FT} = 0.38\frac{P_{FT}P_T t}{\beta_T} \tag{2.2-25}$$

and

$$M_{FD} = 0.38\frac{P_{FD}P_D t}{\beta_D}, \tag{2.2-26}$$

where P_{FT} and P_{FD} are the peak-to-average power ratios in the TFE and driver fuel, respectively. Since the choice of parameters sets R_m, the ratio of the driver fuel to TFE fuel mass for fuel damage considerations must also equal R_m; consequently, if M_{FD} / $M_{FT} \leq R_m$, then M_{FT} will determine the fuel mass based on fuel damage requirements. For this condition,

$$\left(\text{for } \frac{M_{FD}}{M_{FT}} \leq R_m, \text{ and } M_{FT} > M_{ET}\right) \qquad M_{FD} = M_{FT}R_m. \tag{2.2-27}$$

If M_{FD} / $M_{FT} > R_m$, then M_{FT} will determine the fuel mass based on fuel damage requirements. For this condition,

$$\left(\text{for } \frac{M_{FD}}{M_{FT}} > R_m, \text{ and } M_{FD} > M_{ED}\right) \qquad M_{FT} = \frac{M_{FD}}{R_m}. \tag{2.2-28}$$

The total fuel mass, based on fuel damage considerations, M_F, is

$$M_F = M_{FT} + M_{FD}. \qquad (2.2\text{-}29)$$

2.2.3.3 Fuel Mass Based on Thermionic/Thermal Power Considerations

Thermal and thermionic requirements are interrelated. The first step is to compute the volume-adjusted thermal resistance of the fuel pellet. The volume-adjusted thermal resistance for an annular fuel pellet, R_f^T, is given by

$$R_f^T = \frac{r_f^2(Z^2 - 1 - 2\ln Z)}{4k_f Z^2}, \qquad (2.2\text{-}30)$$

where Z is the ratio of the outer to inner TFE fuel pellet diameter and k_f is the thermal conductivity of the fuel pellet.

Next, the required emitter surface area, A_T, and the total heat flux, Q'', across the emitter is computed.

$$A_T = \frac{P}{\phi}, \text{ and} \qquad (2.2\text{-}31)$$

$$Q'' = \phi/e \, . \qquad (2.2\text{-}32)$$

where ϕ is the maximum net electrical power flux at the emitter surface, and e is the net efficiency. The calculated peak fuel temperature, T_f^c, is

$$T_f^c = T_e + \frac{2\,Q''\,r_e\,R_f^T}{r_f^2\left(1 - 1/Z^2\right)} \qquad (2.2\text{-}33)$$

where T_e is the desired emitter temperature. It has been assumed for simplicity that the emitter and fuel surface temperatures are almost equal. The computed peak fuel temperature, T_f^c, is then compared with the maximum allowed fuel temperature, T_f, to ensure that $T_f \geq T_f^c$. If $T_f^c > T_f$, the solution is invalid and a new set of design parameters must be selected. If $T_f \geq T_f^c$, then the required fuel mass for thermal/thermionic considerations, $M_{Th\,T}$, is computed

$$M_{Th\,T} = \left(1 - \frac{1}{Z^2}\right) \rho_{fT}\, r_f^2\, A_T / 2 r_e \ . \tag{2.2-34}$$

Because the driver fuel surface temperature will be ~1000 K lower than the TFE fuel surface temperature and the driver fuel pin diameter can be much smaller, the thermal power limits can be assumed to be controlled by the TFE fuel only. The mass of the driver fuel required for thermal/thermionic considerations is

$$M_{Th\,D} = M_{Th\,T}\, R_m. \tag{2.2-35}$$

The total fuel mass for thermal/thermionic considerations, M_{Th}, is

$$M_{Th} = M_{Th\,T} + M_{Th\,D}. \tag{2.2-36}$$

2.2.4 Limiting Fuel Mass

Because the fuel mass based on critical mass and fuel damage consists of minimum values, and the final mass based on thermal/thermionic requirements is fixed for a particular choice of design parameters, the limiting fuel mass is computed as follows:

If $M_{Th} \geq M_E$, and $M_{Th} \geq M_F$, then

$$M_L = M_{Th}. \tag{2.2-37}$$

If $M_{Th} < M_E$, or $M_{Th} < M_F$, then the solution is invalid and a new set of design parameters must be selected.

2.2.5 Reactor Component Mass Calculations

2.2.5.1 Moderator Mass Calculation

The volume of the TFE region of the core, V_T, is

$$V_T = \frac{M_L}{VF_c\, \rho_{fT}}, \tag{2.2-38}$$

and the moderator volume, V_M, is

$$V_M = \left(\frac{r_D^2 - r_t^2}{r_t^2}\right) V_T. \tag{2.2-39}$$

The moderator mass, M_M, is then given by

$$M_M = \rho_M V_M, \tag{2.2-40}$$

where ρ_M is the moderator density, and the total core volume is

$$V = (V_T + V_M)(1 + VF_{SH}). \tag{2.2-41}$$

2.2.5.2 Structural Mass Calculation

The structural mass, M_s, is computed from

$$M_s = (\rho_{ST} V_T + \rho_{SM} V_M) + 2367V, \tag{2.2-42}$$

where ρ_{ST} and ρ_{SM} are the core average densities of the TFE and the moderator/driver region structure, respectively. The second term (2637) roughly accounts for miscellaneous structure and fuel pin hardware (excluding thermionic structure). The average structural density of 2367 is based on data for the SP-100 reactor (Section 2.1.5.1). Although the pin structure and miscellaneous hardware for the TFE reactor will be different from the structure for the SP-100 reactor, the value of 2637 is assumed to be a reasonable allowance for these components.

2.2.5.3 Reflector Mass Calculation

The core diameter, D, and length, L, are obtained from

$$D = \left(\frac{4V}{a\pi}\right)^{1/3} \tag{2.2-43}$$

and

$$L = aD. \tag{2.2-44}$$

The reflector mass, M_{Rf}, is then

$$M_{Rf} = \pi\rho_{Rf}T[D^2(a + 0.2) + DT(a + 2) + 2T^2], \tag{2.2-45}$$

where T is the reflector thickness. This equation is based on the assumption of an annular reflector surrounding the core and axial reflectors at both ends of the fuel pins. The axial reflectors make up approximately 40 percent of the radial cross section area of the core region.

2.2.5.4 Pressure Vessel Mass Calculation

As for the LMR model (Section 2.1.5.3),

$$r_{pv} = F_{rp}\left(\frac{D}{2} + nT\right), \tag{2.2-46}$$

$$L_{pv} = F_{Lp}L, \tag{2.2-47}$$

$$t_{pv} = \frac{3P_r r_{pv}}{U_s} \tag{2.2-48}$$

if $t_{pv} < t_{\min}$, then set

$$t_{pv} = t_{\min}\ , \tag{2.2-49}$$

$$M_{pv} = 6\pi r_{pv}\rho_{pv}t_{pv}(r_{pv} + L_{pv}). \tag{2.2-50}$$

Note that no plenum length is accounted for in this calculation since it is assumed that the fission gas is purged to an external storage tank.

2.2.5.5 Coolant Mass Calculation

The total reactor volume, V_R, is given by

$$V_R = \pi\left[F_{rp}\left(\frac{D}{2} + T\right)\right]^2 L_{pv}. \tag{2.2-51}$$

Assuming that 20 percent of the reactor contains NaK coolant, the total NaK coolant mass, M_{NK}, in the reactor is

$$M_{NK} = 148\,V_R\ . \tag{2.2-52}$$

2.2.6 Total Reactor Mass

The total reactor mass, M_R, is the sum of the fuel mass and the reactor-component masses (moderator mass, structural mass, reflector mass, pressure vessel mass, and coolant mass):

$$M_R = M_L + M_M + M_s + M_{Rf} + M_{pv} + M_{NK}\ . \tag{2.2-53}$$

2.2.7 Mass Calculations for Ancillary Systems

2.2.7.1 Instrumentation and Control Mass Calculation

As in Section 2.1.7.1, for the SP-100 reactor, the instrumentation and control mass, M_{IC}, is computed from the effective core area, A, and payload separation distance, R_p:

$$A = \left(\frac{2V}{\pi}\right)^{2/3} \tag{2.2-54}$$

$$M_{IC} = d_1 + d_2 A + d_3 R_p \,. \tag{2.2-55}$$

2.2.7.2 Safety System Mass Calculation

As for the LMR model (Section 2.1.7.2),

$$r_{\text{eff}} = \left(\frac{3V}{4\pi}\right) 1/3 \,, \tag{2.2-56}$$

$$M_{MS} = 248 r_{\text{eff}} \,, \tag{2.2-57}$$

and

$$M_{SR} = 389 r_{\text{eff}} \,, \tag{2.2-58}$$

where the constants (248 and 389) for the miscellaneous safety systems mass, M_{MS}, and the safety rod mass, M_{SR}, respectively, in Equations (2.2-57) and (2.2-58) were obtained from the values for the SP-100 reactor. Although these quantities will not be identical for the TFE reactor (in fact, the safety system may be entirely different), the values are used to provide an allowance for safety system mass that would be comparable to the values for the LMR concept. Similarly, we have assumed a reentry heat shield, as in Section 2.1.7.2:

$$M_{NC} = 1.6(222 r_{pv}^2 - 1.75 r_{pv}) \,, \tag{2.2-59}$$

$$R_a = r_{pv} + 0.0177 \,, \tag{2.2-60}$$

$$R_b = R_a + 0.0059 \,, \tag{2.2-61}$$

$$\theta = \tan^{-1}\left[\frac{D_{\text{pay}}/2 - (r_{pv} + T)}{L_{pv} - 0.21 + R_p}\right] \,, \tag{2.2-62}$$

$$R_c = r_{pv} + L_{pv} \tan\theta \,, \tag{2.2-63}$$

$$R_d = R_c + 0.0059, \quad (2.2\text{-}64)$$

$$M_{CS} = 1600(L_{pv} - r_{pv})[R_b^2 + R_b R_d + R_d^2) - (R_a^2 + R_a R_c + R_c^2)], \quad (2.2\text{-}65)$$

and the total heat shield mass, M_{HS}, is

$$M_{HS} = M_{NC} + M_{CS}. \quad (2.2\text{-}66)$$

The total safety system mass, M_{SS}, is

$$M_{SS} = M_{MS} + M_{SR} + M_{HS}. \quad (2.2\text{-}67)$$

2.3 Out-of-Core Thermionic Reactors

2.3.1 Reactor Description

The STAR-C reactor concept proposed by General Atomics (GA, 1987a) was chosen to be representative of out-of-core thermionic reactor concepts for this model development effort. STAR-C (Figure 2-12) uses a solid core composed of segmented, annular fuel plates that are supported by graphite trays. Each fuel plate is made up of six pie-shaped, uranium dicarbide segments fully enriched in uranium-235. The graphite trays are coated with niobium carbide to suppress carbon vaporization, which could result in carbon attack on the emitters of the thermionic devices. The reactor core is built by stacking the graphite trays and fuel plates, with the number of fuel-tray assemblies being dictated by the axial power level. A 10-kWe system has a core that is approximately 26 cm in diameter and 48 cm long. The thickness of the trays can be varied to improve the uniformity of the axial power profile. Heat generated in the reactor core is conducted radially outward to the core surface where it is radiated to thermionic devices surrounding the core. During operation, the maximum core and core-surface temperatures are expected to be approximately 2300 K and 2000 K, respectively.

The thermionic devices, which are located in the radial reflector, collect heat radiated across a gap from the core. The nominal operating temperature of the emitter is 1860 K. The collector is cooled by an integral heat pipe that conducts heat to the system radiator surrounding the reactor. The radiator is sized so that the collector operating temperature is 1000 K. Under these conditions, the efficiency of the thermionic devices is approximately 14 percent. When the other electrical losses are considered, the overall system efficiency is approximately 12 percent.

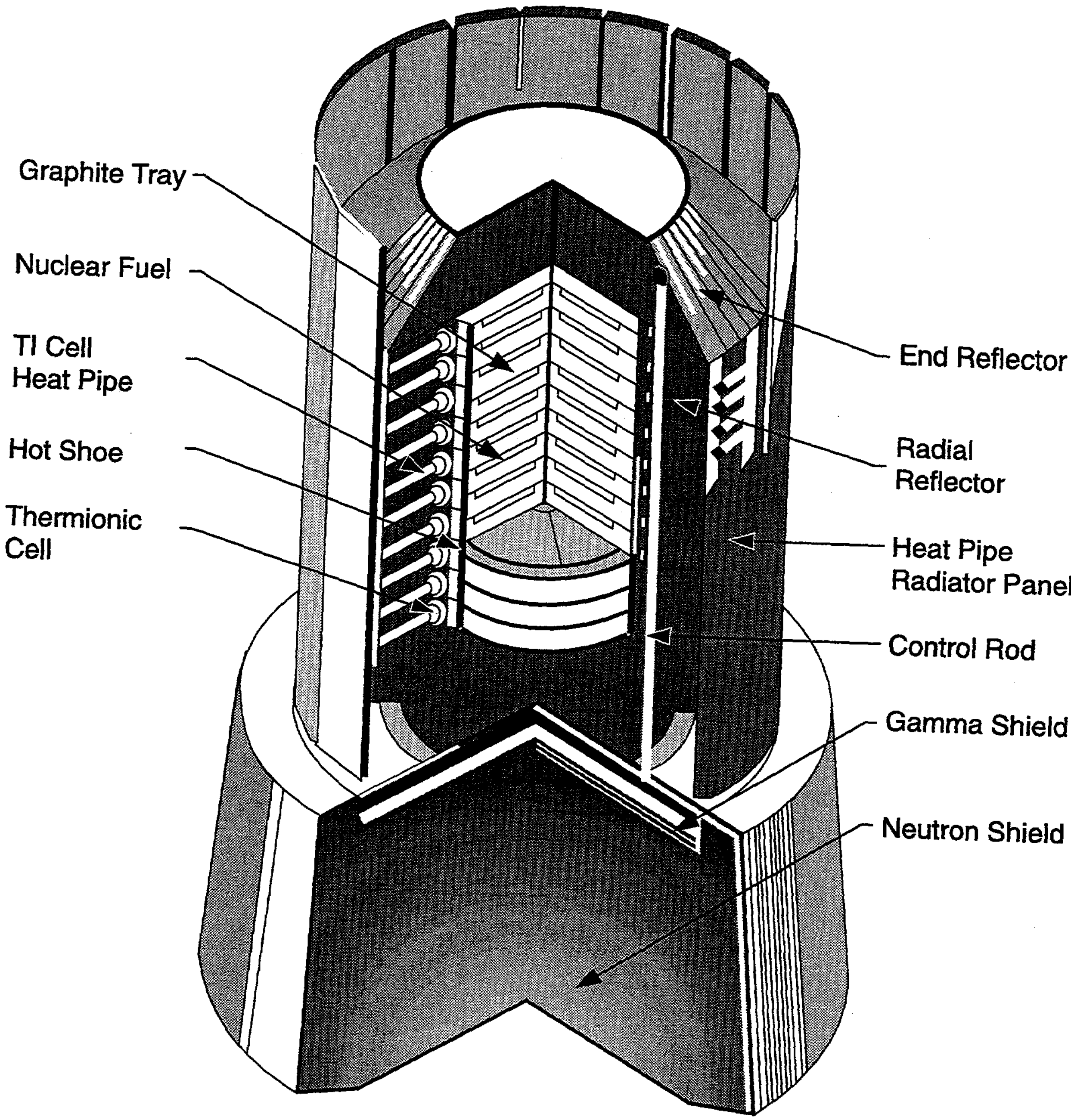

Figure 2-12. STAR-C space nuclear reactor (GA, 1987a).

Reactor control is accomplished by movable rods located in the radial reflector. The rods consist of a boron carbide poison section and a beryllium reflector section. When the reactor is shut down, the poison section of the rod is located in the reflector. To start the reactor, the rods are moved upward to place the beryllium section in the reflector.

Radiation protection for the payload is provided by a separation boom, a lithium hydride neutron shield, and a zirconium hydride gamma shield. The boom length and shield thicknesses are optimized based on system mass.

2.3.2 General Approach

The general approach for the OTR model is similar to that used for the LMR and TFE models; however, some aspects of the optimization scheme are different. For example, increasing the core aspect ratio, *a*, not only helps reduce shield size and mass, it will also increase the surface area for thermionic devices and reduce the conductive path length for heat energy through the fueled region to the reactor surface. These benefits, resulting from large aspect ratios, often outweigh the penalty of increased critical mass and can result in very large optimum aspect ratios. Mechanical/structural considerations will probably place an upper limit on the aspect ratio, but at present a defensible choice for the maximum aspect ratio has not been determined.

The proposed STAR-C reactor uses UC_2 annular fuel regions in graphite trays, so that the central region of the core consists of an unfueled graphite cylinder. The ratio of the diameter of the unfueled region to the outer diameter of the core, *b*, will affect the critical mass and power density. Hence, *a* and *b* are varied in the optimization scheme to obtain the minimum reactor and shield system mass. As with the preceding models, values are selected for the variable parameters (in this case, *a* and *b*). The computation sequence described in the remainder of Section 2.3 and in Section 3.4 is executed to compute the reactor and shield mass, respectively. The computation is then repeated for all allowed combinations of design parameters.

Don Gallup of Sandia National Laboratories has incorporated this OTR model into an overall power system code. He has also enhanced the capability of the model by allowing the core surface temperature, the emitter temperatures, and the thermionic efficiency to be variables (Gallup, 1990).

2.3.3 Fuel Mass Calculations

2.3.3.1 Fuel Mass Based on Fuel Damage Considerations and Required Core Surface Area

Some quantities will not change during the optimization procedure and are computed first; they include:

- the quantity of fuel required for fuel burnup,

$$M_B = \frac{0.38Pt}{\varepsilon e}, \qquad (2.3\text{-}1)$$

- the quantity of fuel required to stay within fuel damage limits,

$$M_F = \frac{0.38P_F Pt}{\beta e}, \qquad (2.3\text{-}2)$$

[These two expressions are identical to those used to calculate fuel burnup and fuel damage for liquid-metal-cooled reactors; see Equations (2.1-1) and (2.1-3).]

- the core surface area, A_T, required for thermionics,

$$A_T = \frac{P}{\phi f_e}, \qquad (2.3\text{-}3)$$

where f_e is the maximum fraction of the core surface area available as emitter surface.

2.3.3.2 Fuel Mass Based on Neutronic Considerations

The volume fraction of the fuel and moderator, VF, is computed for the selected ratio of the inner diameter of the fuel region to the outer diameter of the core, b:

$$VF_F = (\alpha^2 - b^2)VF_{f^F}, \qquad (2.3\text{-}4)$$

$$VF_M = (1 + b^2 - \alpha^2) + (\alpha^2 - b^2)VF_{f^M}, \qquad (2.3\text{-}5)$$

(VF_M must be > 0.0)

and

$$VF = VF_F + VF_M, \qquad (2.3\text{-}6)$$

where VF_F is the volume fraction of uranium-235 in the core, VF_{f^F} is the volume fraction of uranium-235 in the annular fuel region, VF_{f^M} is the volume fraction of moderator in the annular fuel region, VF_M is the volume fraction of moderator in the core, α is the ratio of the fuel annulus outer diameter to the total core diameter, and VF_{f^M} is the volume fraction of moderator in the annular fuel region.

The core-averaged moderator-to-fuel molecular ratio (R = carbon atoms/uranium-235 atoms) is computed next:

$$R = 21.6\left(\frac{\rho_M}{\rho_F}\right)\left(\frac{VF_M}{VF_F}\right) \tag{2.3-7}$$

where ρ_F is the fuel density, ρ_M is the moderator density, and 21.6 is the ratio of the molecular weight of UC_2 to the atomic weight for carbon.

The critical mass of uranium-235 for compacted, reflected spheres of UC_2 was computed for a variety of moderator-to-fuel ratios, R. The UC_2 was assumed to be 93 percent enriched and a 10-cm-thick beryllium reflector was used in the calculations. These critical mass values were obtained using the FEMP1D neutron transport code (McDaniel and Harris, 1983). The results from these calculations are given in Table 2-4 and are plotted in Figure 2-13. Table 2-4 is used to obtain the compacted critical mass of uranium-235, M_C^C, for the computed moderator-to-fuel ratio.

The next step is to compute the critical mass correction for the effect of a cylindrical reactor of aspect ratio a. As with the preceding models,

$$C_a = \frac{1}{3}(2.34a^{2/3} + a^{-4/3}) \qquad \text{for } a \geq 1.0 \tag{2.3-8}$$

and

$$C = C_a C_m. \tag{2.3-9}$$

Since OTRs are not compacted critical spheres, the corrections given in Marshall (1986) are used to obtain the initial critical mass, M_C^0:

$$M_C^0 = \frac{0.93 C M_C^C}{\varepsilon^2}\left(\frac{13600}{VF\rho_F}\right)^{1.5} \tag{2.3-10}$$

Table 2-4. M_C^C, Critical Mass of Reflected Compacted UC_2 Spheres as a Function of R (carbon atoms/^{235}U atoms)

R	M_C^C
0.1	18
0.3	19.1
1.0	24.1
1.7	26.4
3.0	32.2
10.0	52.4
17.0	61.6
30.0	68.6
50.0	70.5
70.0	67.4
100.0	61.8
170.0	49.2
300.0	34.5
1000.0	14.9

The end-of-life critical mass, M_C, is then

$$M_C = \frac{M_C^0 + \sqrt{(M_C^0)^2 + 4M_C^0 M_B(1-\varepsilon)}}{2}, \tag{2.3-11}$$

The total fuel mass based on neutronic limits is then

$$M_E = M_C + M_B. \tag{2.3-12}$$

2.3.3.3 Fuel Mass Based on Thermal/Thermionic Considerations

The required fuel mass based on thermionic considerations is a function of the core surface area. First, the core volume, V, is computed from the required thermionic surface area and the assumed aspect ratio:

$$V = \frac{A_T^{3/2}}{4\sqrt{\pi a}} \tag{2.3-13}$$

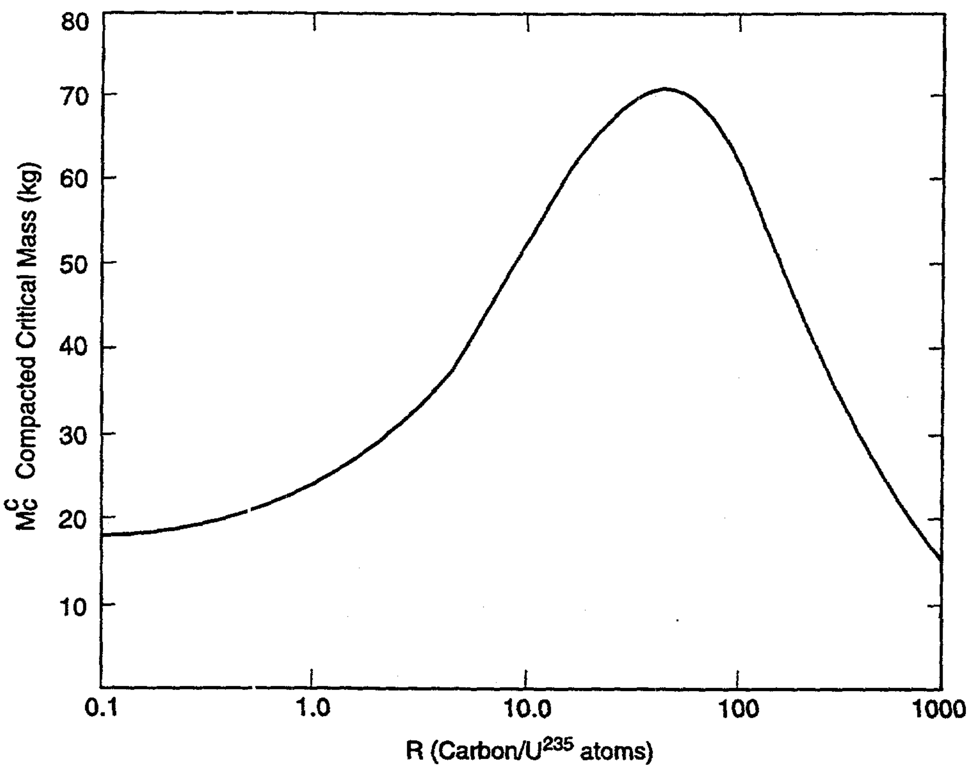

Figure 2-13. Critical mass value.

The upper and lower core ends have not been included as thermionic surfaces. The fuel mass based on thermal/thermionic requirements, M_{Th}, is

$$M_{Th} = \frac{\rho_F V \, VF_F}{\varepsilon}. \tag{2.3-14}$$

The next step is to ensure that fuel temperature limits are not exceeded. The core diameter D is computed next in order to obtain the volume-adjusted thermal resistance:

$$D = \left[\frac{4V}{a\pi\left(1 - b^2\right)} \right]^{1/3} . \tag{2.3-15}$$

Heat is transferred from the fuel to the core surface by conduction through the fuel and outer graphite annulus. A limit on the allowed fuel temperature will constrain the core power density and the minimum allowed fuel mass.

The volume-adjusted thermal resistance of the fuel, R_f^T, can be expressed as

$$R_f^T = \frac{D^2}{8k_f} \left[\frac{\alpha^2 - b^2}{2} - b^2 \ln\left(\frac{\alpha}{b}\right) \right], \tag{2.3-16}$$

where k_f is the thermal conductivity of the fuel, and D is the core outer diameter. The volume-adjusted thermal resistance of the outer graphite annulus, R_c^T, is given by

$$R_c^T = \frac{D^2}{8k_c}\left(\alpha^2 - b^2\right)\ln\left(\frac{1}{\alpha}\right), \tag{2.3-17}$$

where k_c is the conductivity of the graphite annulus, and

$$R_T^T = R_f^T + R_c^T . \tag{2.3-18}$$

R_T^T is the total volume-adjusted thermal resistance from the core inside diameter to the core surface.

The heat flux Q'', across the emitter, is

$$Q'' = \phi/e . \tag{2.3-19}$$

The maximum value calculated for the fuel temperature T_f^c, is

$$T_f^c = \frac{4Q''R_T^T}{D\left(\alpha^2 - b^2\right)} + T_{cs} \tag{2.3-20}$$

where T_{cs} is the specified core surface temperature. The computed peak fuel temperature, T_f^c, is then compared with the maximum allowed fuel temperature, T_f, to ensure that $T_f \geq T_f^c$. If $T_f^c > T_f$, the solution is invalid and a new set of design parameters must be selected. If $T_f \geq T_f^c$, then the solution is valid and the required fuel mass for thermal/thermionics must be compared with the fuel mass requirements for neutronics and fuel damage limits.

2.3.4 Limiting Fuel Mass

If $M_{Th} \geq M_E$, and $M_{Th} \geq M_F$, then

$$M_L = M_{Th} \tag{2.3-21}$$

If $M_{Th} < M_E$, or $M_{Th} < M_F$, then the solution is invalid and a new set of design parameters must be selected.

2.3.5 Reactor Component Mass Calculations

2.3.5.1 Moderator Mass Calculation

The moderator mass is given by

$$M_M = \varepsilon M_L R\left(\frac{1}{21.6}\right). \tag{2.3-22}$$

The moderator plus fuel mass (M_T) is

$$M_T = M_L + M_M, \tag{2.3-23}$$

with a combined density, ρ_T, given by

$$\rho_T = \frac{M_T}{\dfrac{M_L}{\rho_F} + \dfrac{M_M}{\rho_M}} \tag{2.3-24}$$

where ρ_F is the unhomogenized fuel density and ρ_M is the moderator density. The core volume is then

$$V = \frac{M_T}{VF\rho_T}. \tag{2.3-25}$$

2.3.5.2 Structural Mass Calculation

Since no fuel pin hardware will be required, the structure for the OTR will consist of miscellaneous structure for core support and other considerations. As with the structural mass calculation for the in-core thermionic reactor, an allowance for the miscellaneous structure, estimated from the miscellaneous structural mass density for SP-100, gives a structural mass for the OTR, M_s, as:

$$M_s = (1183 + \rho_s)V. \tag{2.3-26}$$

Even though the SP-100 is an LMR, its reference design is used as a basis for arriving at reasonable mass estimates for the reactor and ancillary components of the OTR (see Section 1.3). The ρ_s term in Equation (2.3-24) is provided to allow for additional structure, should the need for it become apparent as the design evolves. At present, ρ_s is assumed to be zero.

2.3.5.3 Reflector Mass Calculation

The reflector mass is computed assuming that the core is surrounded on all sides by a reflector of thickness T. The reflector mass, M_{Rf}, is then

$$M_{Rf} = \pi\rho_{Rf}T\left[D^2\left(a+\frac{1}{2}\right)+DT(a+2)+2T^2\right] \tag{2.3-27}$$

where ρ_{Rf} is the reflector density.

2.3.6 Total Reactor Mass

Since this OTR concept does not require a pressure vessel or coolant, the total reactor mass, M_R, is the sum of the fuel mass and the reactor component masses (moderator mass, structural mass, and reflector mass).

$$M_R = M_L + M_M + M_s + M_{Rf}. \tag{2.3-28}$$

2.3.7 Mass Calculations for Ancillary Systems

2.3.7.1 Thermionic Mass Calculation

The mass of the thermionic devices (known as SET devices) is directly proportional to the reactor power. The thermionic device mass, M_{SET}, can then be computed as

$$M_{SET} = U_t P \tag{2.3-29}$$

where U_t is a constant of proportionality.

2.3.7.2 Radiator Mass Calculation

The radiator mass, M_{RAD}, can be expressed as a linear function of the reactor thermal power:

$$M_{RAD} = \frac{U_r P}{e}, \tag{2.3-30}$$

where U_r is a constant of proportionality.

2.3.7.3 Instrumentation and Control Mass Calculation

As with the previously described models, the instrumentation and control mass, M_{IC}, is computed from the effective core area, A, and the payload separation distance, R_p.

$$A = \left(\frac{2V}{\pi}\right)^{2/3} \tag{2.3-31}$$

and

$$M_{IC} = d_1 + d_2 A + d_3 R_p. \tag{2.3-32}$$

2.3.7.4 Safety System Mass Calculation

As with the SP-100 reactor (Section 2.1.7.2),

$$r_{\text{eff}} = \left(\frac{3V}{4\pi}\right)^{1/3}. \tag{2.3-33}$$

and

$$M_{SR} = 389 r_{\text{eff}}, \tag{2.3-34}$$

No miscellaneous safety mass was included since no auxiliary cooling loop is required and the safety rods in conjunction with the tungsten hot shoe/emitter surrounding the core were assumed to be sufficient to prevent flooded criticality. The safety rods were assumed to be located in the unfueled region in the center of the core; hence, no volume allowance for safety rods was assumed.

In its proposed configuration, the radiator surrounds the core; consequently, the reentry heat shield could not also surround the reactor during operation. A retractable heat shield or some other form of reentry protection may be required. For this model, a reentry heat shield of the type used for SP-100 will be assumed as a mass allowance for reentry protection. The mass of the reentry heat shield is computed as follows:

$$M_{NC} = 1.6\left[222\left(\frac{D}{2}\right)^2 - 1.75\frac{D}{2}\right], \qquad (2.3\text{-}35)$$

$$R_a = \frac{D}{2} + 0.0177, \qquad (2.3\text{-}36)$$

$$R_b = R_a + 0.0059, \qquad (2.3\text{-}37)$$

$$L = aD, \qquad (2.3\text{-}38)$$

$$\theta = \tan^{-1}\left[\frac{(D_{pay}/2) - (D/2)}{L + T + R_p}\right], \qquad (2.3\text{-}39)$$

$$R_c = \frac{D}{2} + L\tan\theta, \qquad (2.3\text{-}40)$$

$$R_d = R_c + 0.0059, \qquad (2.3\text{-}41)$$

$$M_{CS} = 1600\left(L - \frac{D}{2}\right)[(R_b^2 + R_b R_d + R_d^2) - (R_a^2 + R_a R_c + R_c^2)]. \qquad (2.3\text{-}42)$$

The total heat shield mass, M_{HS}, is

$$M_{HS} = M_{NC} + M_{CS}. \qquad (2.3\text{-}43)$$

The total safety system mass is

$$M_{SS} = M_{SR} + M_{HS}. \qquad (2.3\text{-}44)$$

THIS PAGE INTENTIONALLY LEFT BLANK

3. RADIATION-SHIELDING MODELS

The radiation-shielding models provide estimates of the radiation shield thicknesses and mass, the dose at the outer shield surface, and the mass of the payload separation boom.

3.1 General Approach

3.1.1 Gamma Shielding Requirements

From Appendix 4 of Marshall (1986), the gamma dose at the payload from the reactor, D_g, has the approximate functional relationship given by

$$D_g = \frac{B N_s E e^{-\mu t_s}}{\mu_c e L R_p^2}, \tag{3.1-a}$$

where B is the buildup factor, N_s is a proportionality constant, E is the electrical energy at the payload [see Appendix 4 of Marshall (1986)], e is the net fractional efficiency, t_s is the shield thickness, μ is the gamma attenuation coefficient, μ_c is the core self-absorption coefficient, and L is the core length. For the original RSMASS model (Marshall, 1986), the proportionality constant N_s was obtained for one type of shield (tungsten/lithium hydride), one type of reactor (LMR), and one power level; the proportionality constant was assumed to be generally applicable to all concepts. This is a fair assumption for the last two considerations (same reactor type and power level), but it is inappropriate to use the LMR-tungsten/lithium hydride proportionality constant for other shield materials. Furthermore, fair agreement for different reactor types and power levels, while acceptable for large, multimegawatt systems, is not adequate for low-power systems, for which RSMASS-D was developed.

The shielding model can be improved by noting that the quantity $BN_s e^{-\mu t_s}/\mu_c$ can be made equivalent to two factors:

$$N_{og} A_g = \frac{B N_s e^{-\mu t_s}}{\mu_c}, \tag{3.1-b}$$

where N_{og} is the proportionality factor for a reference set of conditions, and A_g is the attenuation parameter for deviations from the reference conditions. Therefore, deviations in shield thickness, reactor type and composition, and shield materials are all accounted for by A_g.

The values for A_g are determined by performing spherical transport calculations for the reference SP-100 reactor and for other cases of interest, including a range of shielding thicknesses, shielding materials, and a variety of reactor types. The ratio of the dose at some dose plane for the case of interest to the dose for the reference SP-100 case provides the values of A_g for each case. (The procedure for obtaining the attenuation coefficients is described in more detail in Appendix C.)

The results of these calculations provide an A_g matrix for each reactor/shield concept, with the elements of each matrix corresponding to various thicknesses of neutron and gamma shield materials. The values of the elements of the A_g matrix for the LMR, in-core TFE reactor, and OTR shielding models are provided in Appendix C. Figure 3-1 also provides (for the purpose of illustration) a plot of A_g as a function of neutron shield thickness for a variety of gamma shield thicknesses for the OTR.

Before obtaining the proportionality constant N_{og}, one further improvement to the model must be explained. The $1/R_p^2$ factor, used to account for geometry attenuation (i.e., attenuation by virtue of separation distance between the reactor and the payload) in the original model, is based on a point-source assumption. This assumption yields good agreement with the actual geometric attenuation for distances greater than 1 m. Good agreement for distances less than 1 m can be obtained by assuming a disk source. It can be shown that the gamma or neutron flux at any location is the integral of the point-attenuation kernel, *G(r)*, over the surface of the disk. For geometric attenuation for a point source,

$$G(r) = \frac{1}{r^2}. \quad (3.1\text{-c})$$

Since $dA \sim r\,dr$, the relative change in dose as a function of payload distance, R_p, is then given by

$$\int_{R_p}^{\sqrt{R_p^2 + 0.75^2}} \frac{1}{r}\,\mathrm{dr} = \ln\sqrt{R_p^2 + 0.75^2} - \ln R_p, \quad (3.1\text{-d})$$

where 0.75 m in Equation (3.1-d) is the maximum shield radius for the reference case.

Thus, the expression for the payload dose for gamma radiation, D_g, becomes

$$D_g = \frac{N_{og} A_g E}{eL}(\ln\sqrt{R_p^2 + 0.75^2} - \ln R_p). \quad (3.1\text{-e})$$

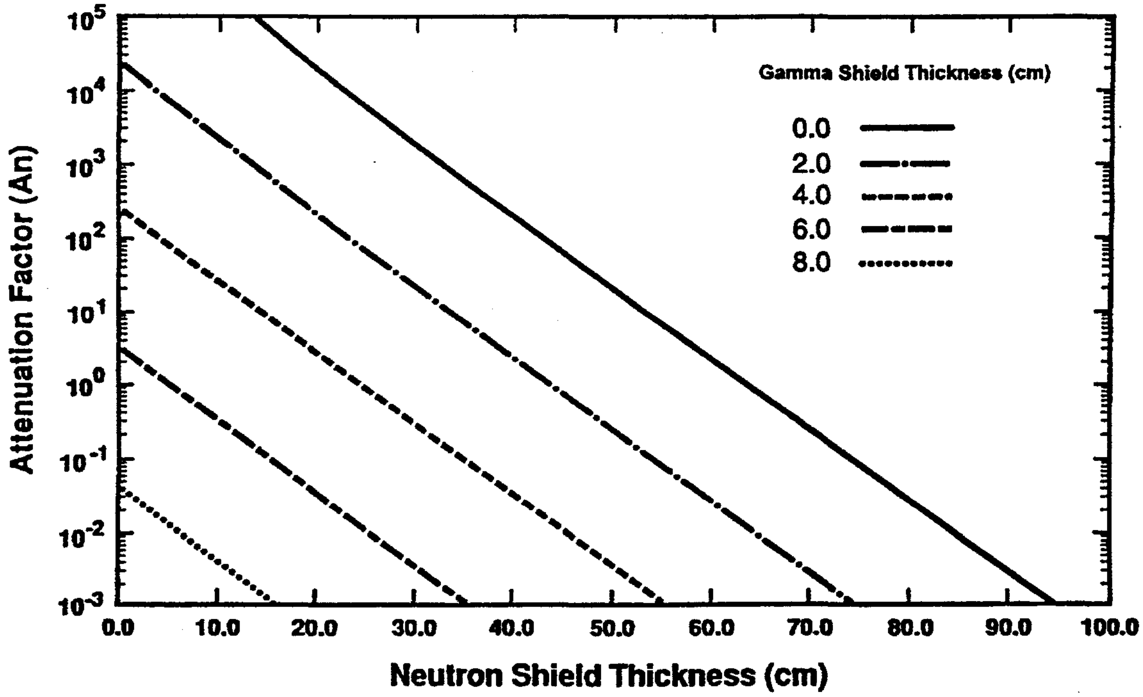

Figure 3-1. A_n Matrix: shield neutron-attenuation factor (A_n) as a function of neutron shield thickness for a variety of gamma shield thicknesses for the OTR.

Transposing terms, we can now obtain an expression for N_{og},

$$N_{og} = \frac{D_g eL}{A_g E}(\ln\sqrt{R_p^2 + 0.75^2} - \ln R_p)^{-1}. \tag{3.1-f}$$

The value for N_{og} is determined by substituting the appropriate quantities into this expression. These quantities were obtained from detailed calculations for the reference (SP-100) case (GE, 1987). $A_g = 1.0$ for the reference case. The proportionality constant, N_{og}, is found to be

$$N_{og} = 2 \times 10^7. \tag{3.1-g}$$

The required A_g can now be computed by rearranging Equation (3.1-e) and substituting the value for N_{og}, thus obtaining

$$A_g = \frac{D_g eL}{(2 \times 10^7)E}(\ln\sqrt{R_p^2 + 0.75^2} - \ln R_p)^{-1}. \tag{3.1-h}$$

Hence, the above equation is used to compute the required A_g, and the matrixes in Appendix C provide the required combination of shield thicknesses to yield the required A_g. In these equations it is assumed that the gamma source is directly proportional to the total reactor system energy. Most of the gamma radiation is from fission gammas, rather than activation products. Since the fission gamma dose and the number of fissions is directly proportional to reactor energy, the assumption implicit in these equations is justified.

3.1.2 Neutron Shielding Requirements

The approach used to compute gamma shielding requirements can also be used to compute neutron shielding requirements. The neutron dose, D_n, however, is directly proportional to the neutron flux, and the neutron flux in turn is proportional to the total energy divided by the fuel atom density (Marshall, 1989). If the fuel atom density for the case being considered deviates significantly from the value assumed to obtain the neutron attenuation parameter, A_n, some error will be produced by adopting an equation of the form (3.1-h) for neutrons. Although this error is expected to be small, the correction for the actual fuel density can easily be incorporated into the equation for the required neutron attenuation, A_n. The equation for A_n is given by

$$A_n = \frac{D_n e L M_L}{(1.57 \times 10^{20}) V E N_{235}} \left(\ln \sqrt{R_p^2 + 0.75^2} - \ln R_p\right)^{-1}, \tag{3.1-i}$$

where M_L / V is the fuel density for the case under consideration, N_{235} is the atom density assumed to obtain the tabulated values of A_n, and the quantity 1.57×10^{20} is the product of the normalization constant and the conversion factor required to convert fuel density to fuel atom density. As with A_g, the procedure for obtaining the neutron attenuation parameters is described in more detail in Appendix C, and the results of these calculations provide an A_n matrix.

3.2 LMR Radiation Shielding

3.2.1 Shield Mass Calculation

The shield geometry and materials for the LMR model are similar to the shield for the reference SP-100 concept. Tungsten is used for the gamma shield, and lithium hydride is used for the neutron shield. A 0.7-cm-thick layer of beryllium is also used for heat conduction. The radiation shield geometry assumed for the LMR model is illustrated in Figure 3-2. The following calculation sequence is used to compute the shield mass:

$$r_r = \frac{F_{rp} D}{2} + T \tag{3.2-1}$$

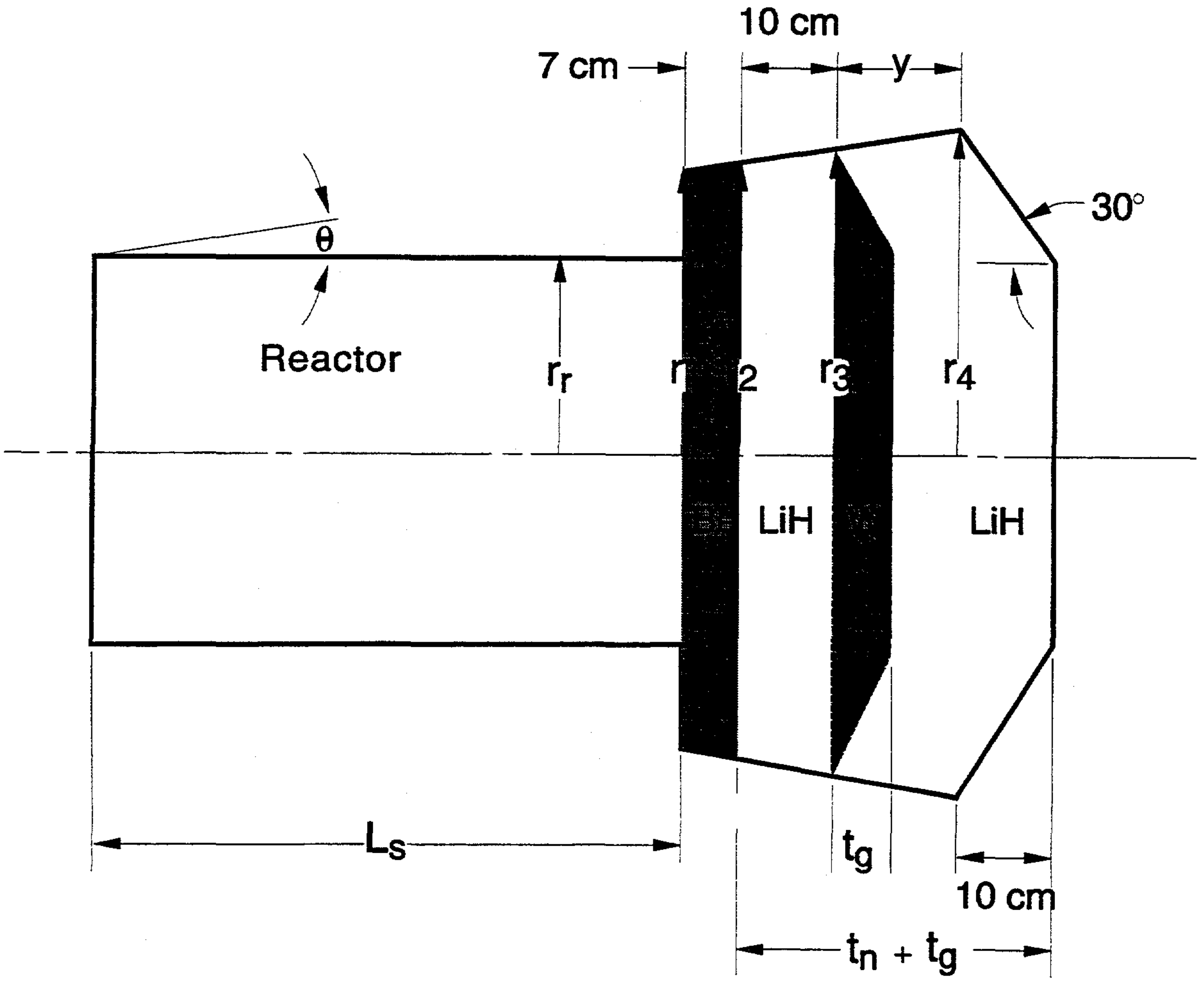

Figure 3-2. Assumed shield geometry for liquid-metal-cooled reactor.

$$L_s = L_{pv} + 0.17, \qquad (3.2\text{-}2)$$

where r_r is the total reactor radius and L_s is the distance from the unshielded end of the pressure vessel to the first gamma shield surface. The required gamma and neutron attenuation factors are computed (A_g and A_n):

$$A_g = \frac{D_g e L}{(2\times 10^7)\,E}\left(\ln\sqrt{R_p^2+0.75^2} - \ln R_p\right)^{-1} \qquad (3.2\text{-}3)$$

and

$$A_n = \frac{D_n e L M_L}{(1.57\times 10^{20})VE(0.0127)}\left(\ln\sqrt{R_p^2+0.75^2} - \ln R_p\right)^{-1}. \qquad (3.2\text{-}4)$$

The core-averaged fuel atom density (0.0127) has been substituted for N_{235} in Equation (3.1-i) to compute A_n for LMRs. The minimum gamma shield thickness (t_{gmin}, an input parameter) is then used with the data given in Tables C-1 and C-2 to obtain the neutron shield thickness (t_{ng} and t_{nn}) required, based on gamma and neutron dose limits respectively; i.e., t_{ng} is obtained from the A_g matrix, and t_{nn} is obtained from the A_n matrix.

The actual neutron shield thickness required, t_n, will be the larger of the two; i.e.,

$$t_n = \text{larger of } t_{ng} \text{ and } t_{nn}. \qquad (3.2\text{-}5)$$

The total reactor shield mass is then computed. The first step is to compute the dimensions of the radii of the conic sections of the shield (see Figure 3.2-1):

$$r_1 = r_r + L_s \tan\theta \qquad (3.2\text{-}6)$$

$$r_2 = r_r + (L_s + 0.007)\tan\theta \qquad (3.2\text{-}7)$$

$$r_3 = r_r + (L_s + 0.17)\tan\theta \qquad (3.2\text{-}8)$$

$$y = \frac{(0.577)(t_g + t_n - 0.1) - L_s\tan\theta}{\tan\theta + 0.577}, \qquad (3.2\text{-}9)$$

$$r_4 = r_r + (L_s + 0.17 + y)\tan\theta \qquad (3.2\text{-}10)$$

If $r_3 > r_4$, then set $r_4 = r_3$ and $y = 0$.

The dimensions corresponding to r_r, r_1, r_2, r_3, r_4, L_{pv}, L_s, t_g, t_n, and θ are shown in Figure 3-2.

Volumes of the conic sections are computed next:

$$V_1 = (0.0733)[r_1^2 + r_1 r_2 + r_2^2], \quad (3.2\text{-}11)$$

$$V_2 = (0.1047)[r_2^2 + r_2 r_3 + r_3^2], \quad (3.2\text{-}12)$$

$$V_{3A} = \pi r_r^2 t_g, \quad (3.2\text{-}13)$$

$$V_{3B} = \frac{\pi t_g}{3}(r_3^2 + r_3 r_r + r_r^2), \quad (3.2\text{-}14)$$

$$V_3 = \frac{(V_{3A} + V_{3B})}{2}, \quad (3.2\text{-}15)$$

$$V_4 = \frac{\pi y}{3}(r_3^2 + r_3 r_4 + r_4^2), \quad (3.2\text{-}16)$$

$$V_5 = \frac{\pi}{3}(t_g + t_n - y - 0.10)(r_4^2 + r_r r_4 + r_r^2). \quad (3.2\text{-}17)$$

The beryllium, gamma, and neutron shield masses (M_{Be}, M_{gs}, and M_{ns}, respectively) are then

$$M_{Be} = 1840 V_1, \quad (3.2\text{-}18)$$

$$M_{gs} = \rho_{gs} V_3, \quad (3.2\text{-}19)$$

$$M_{ns} = \rho_{ns}(V_2 + V_4 + V_5 - V_3). \quad (3.2\text{-}20)$$

where ρ_{gs} and ρ_{ns} are the gamma and neutron shield densities, respectively. The total shield mass, M_{TS}, is then

$$M_{TS} = M_{Be} + M_{gs} + M_{ns}. \quad (3.2\text{-}21)$$

The shield computation is then repeated for all allowed gamma shield thicknesses (as specified in the input), and the gamma shield thickness resulting in the lowest shield mass is selected as the mass-optimized choice.

3.2.2 Dose at Shield Surface

Since some of the control electronics will be located directly behind the radiation shield, the dose at the outer shield surface is of interest. The dose may be easily computed by transposition of the equations derived in Section 3.1.

First, the total shield thickness is computed:

$$T_{TS} = t_g + t_n + 0.07, \quad (3.2\text{-}22)$$

$$T_0 = 0.21, \quad (3.2\text{-}23)$$

$$\Delta T = T_0 + T_{TS}, \quad (3.2\text{-}24)$$

where T_0 is the distance from the core to the nearest shield face, and ΔT is the distance from the core to the outer shield face.

Then the neutron and gamma doses at the shield outer surface (D_{ns} and D_{gs}, respectively) are computed:

$$A_R = \frac{\ln\sqrt{\Delta T^2 + 0.75^2} - \ln \Delta T}{\ln\sqrt{R_p^2 + 0.75^2} - \ln R_p}, \quad (3.2\text{-}25)$$

$$D_{ns} = D_n A_R, \quad (3.2\text{-}26)$$

$$D_{gs} = D_g A_R, \quad (3.2\text{-}27)$$

where A_R is the attenuation reduction factor.

3.2.3 Boom Mass Calculation

The payload dose can be reduced by radiation shielding and by increasing the distance from the core and payload. A boom will be required to separate the payload from the core and to support power transmission lines and instrumentation and control cables. A rough approximation can be made that the boom mass, M_{BM}, is directly proportional to the payload separation distance, R_p:

$$M_{BM} = F_{BM} R_p, \quad (3.2\text{-}28)$$

where F_{BM} is a proportionality constant. This formula can be improved upon by accounting for deployment canister mass and other considerations. For the purposes of RSMASS-D, however, the approach should be adequate for making estimates.

3.3 Radiation Shielding for In-Core Thermionic Reactors

3.3.1 Shield Mass Calculation

For both in-core and out-of-core thermionic reactor concepts, the shield materials and basic geometry proposed by GA (1987a, 1987b) have been assumed. (The shield mass calculation for out-of-core thermionic reactors is provided in Section 3.4.) The radiation shield consists of a zirconium hydride (with 5 wt% natural boron) gamma shield and a lithium hydride neutron shield with the geometry illustrated in Figure 3-3. The shielding model is similar to the model described in Section 3.2 for LMRs.

For the TFE system, the reactor dimensions are:

$$r_r = \frac{F_{rp} D}{2} + T \quad (3.3\text{-}1)$$

and

$$L_s = L_{pv}. \quad (3.3\text{-}2)$$

The required gamma attenuation uses the same formula given for LMRs:

$$A_g = \frac{D_g e L}{(2 \times 10^7) E} (\ln \sqrt{R_p^2 + 0.75^2} - \ln R_p)^{-1}. \quad (3.3\text{-}3)$$

The required A_n will depend on whether a moderator is used; hence

if $T_m = 0.0$,

$$A_n = \frac{D_n e L M_L}{(1.57 \times 10^{20})(0.010) V E} (\ln \sqrt{R_p^2 + 0.75^2} - \ln R_p)^{-1} \quad (3.3\text{-}4)$$

otherwise,

$$A_n = \frac{D_n e L M_L}{(1.57 \times 10^{20})(0.025) V E} (\ln \sqrt{R_p^2 + 0.75^2} - \ln R_p)^{-1}. \quad (3.3\text{-}5)$$

The procedure described in Section 3.2 for obtaining the shield thicknesses is used for the TFE shield, except the matrixes from Tables C-3 and C-4 are used if $T_m = 0.0$, and Tables C-5 and C-6 are used if $T_m \neq 0.0$, to obtain t_{ng} and t_{nn}. As in Section 3.2, the actual neutron shield thickness required, t_n, is the larger of the two:

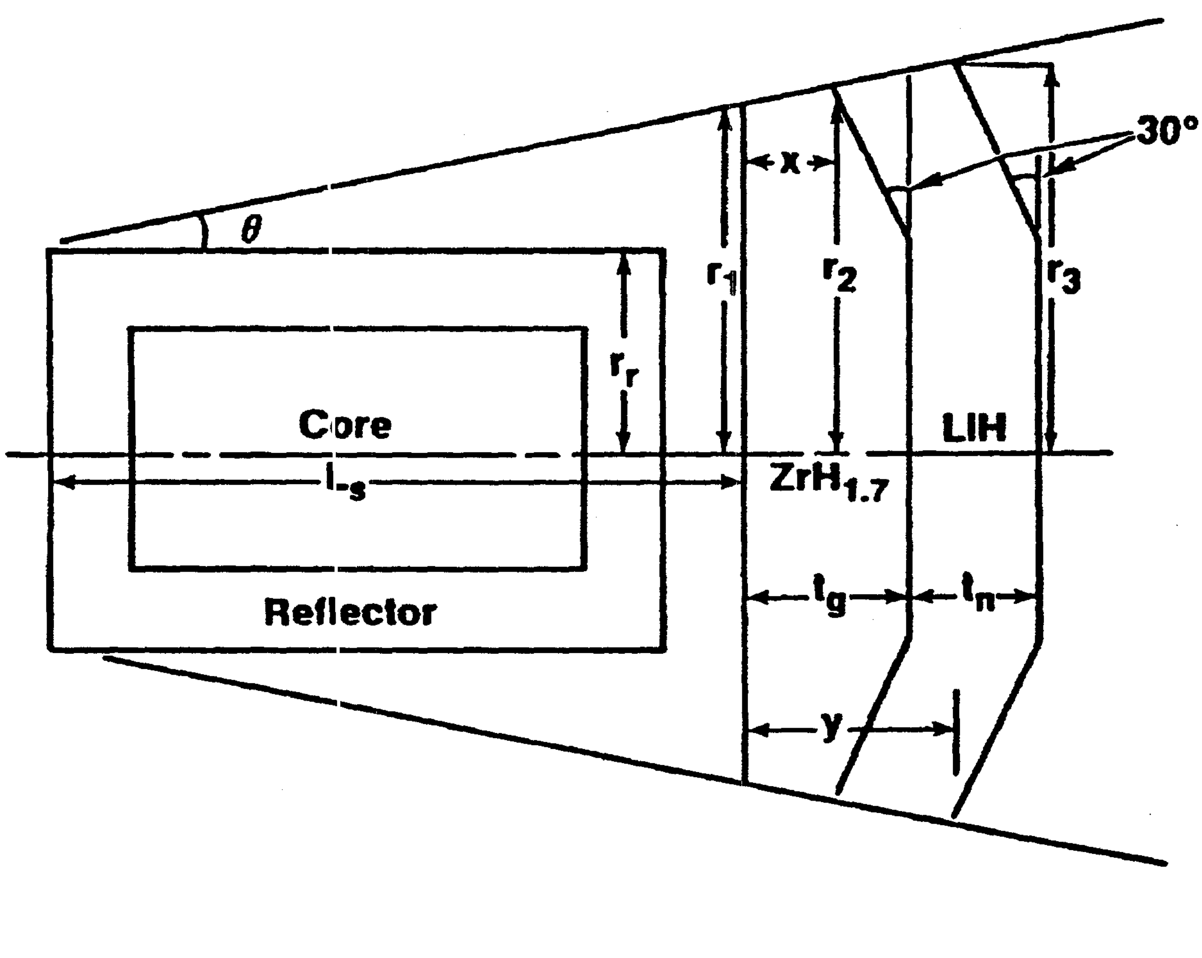

Figure 3-3. Assumed shield geometry for thermionic reactor.

$$t_n = \text{larger of } t_{ng} \text{ and } t_{nn}. \quad (3.3\text{-}6)$$

Next, the shield dimensions are computed (Figure 3-3):

$$x = \frac{(0.577)t_g - L_s \tan\theta}{\tan\theta + 0.577}, \quad (3.3\text{-}7)$$

$$y = \frac{(0.577)(t_g + t_n) - L_s \tan\theta}{\tan\theta + 0.577}, \quad (3.3\text{-}8)$$

$$r_1 = r_r + L_s \tan\theta, \quad (3.3\text{-}9)$$

$$r_2 = r_r + (L_s + x)\tan\theta, \quad (3.3\text{-}10)$$

$$r_3 = r_r + (L_s + y)\tan\theta. \quad (3.3\text{-}11)$$

$$\text{If } r_1 > r_2, \text{ then } r_1 = r_2 \text{ and } x = 0, \quad (3.3\text{-}12)$$

$$\text{If } r_1 > r_3, \text{ then } r_3 = r_1 \text{ and } y = 0. \quad (3.3\text{-}13)$$

The dimensions corresponding to r_r, r_1, r_2, r_3, r_4, L_{pv}, L_s, t_g, t_n, and θ are shown in Figure 3-3.

The volumes are then computed:

$$V_1 = \frac{\pi}{3} x(r_1^2 + r_1 r_2 + r_2^2), \quad (3.3\text{-}14)$$

$$V_2 = \frac{\pi}{3}[(t_g - x)(r_r^2 + r_r r_2 + r_2^2)], \quad (3.3\text{-}15)$$

$$V_3 = \frac{\pi}{3} y(r_1^2 + r_1 r_3 + r_3^2), \quad (3.3\text{-}16)$$

$$V_4 = \frac{\pi}{3}[y(t_g + t_n - y)(r_r^2 + r_r r_3 + r_3^2)], \quad (3.3\text{-}17)$$

and the shield masses are:

$$M_{gs} = \rho_{gs}(V_1 + V_2), \quad (3.3\text{-}18)$$

$$M_{ns} = \rho_{ns}(V_3 + V_4 - V_1 - V_2), \quad (3.3\text{-}19)$$

$$M_{TS} = M_{gs} + M_{ns}. \quad (3.3\text{-}20)$$

3.3.2 Dose at Shield Surface

Here,

$$T_{TS} = t_g + t_n \tag{3.3-21}$$

and

$$T_0 = 0.21. \tag{3.3-22}$$

The remaining equations, which are used to calculate the dose at the outer shield surface for the LMR, are identical to Equations (3.2-24) through (3.2-27).

3.3.3 Boom Mass Calculation

The boom mass for the in-core TFE reactor is calculated in the same manner as that of the LMR [Equation (3.2-28)].

3.4 OTR Radiation Shielding

The out-of-core thermionic reactor shielding model is almost identical to the in-core thermionic reactor shielding model. The exceptions are as follows:

$$r_r = \frac{D}{2} + T, \tag{3.4-1}$$

$$L_s = L, \tag{3.4-2}$$

and

$$A_n = \frac{D_n e L M_L}{(1.57 \times 10^{20})(9.76 \times 10^{-3}) V E} (ln \sqrt{R_p^2 + 0.75^2} - ln\, R_p)^{-1}. \tag{3.4-3}$$

Tables C-7 and C-8 are used to obtain t_{ng} and t_{nn}. For the dose at the shield surface

$$T_0 = 0.15. \tag{3.4-4}$$

4. RESULTS

4.1. Mass Estimate Examples

System mass optimization calculations have been performed using the RSMASS-D models. The reactor and shield masses are presented as a function of electrical power level for the LMR, TFE reactor, and OTR concepts in Figures 4-1, 4-2, and 4-3, respectively. A 7-year operational life has been assumed. The reactor mass also includes safety system and instrumentation and control masses. For the OTR concept, the reactor mass also includes the thermionic and radiator masses. These mass estimates should not be used to determine the advantages of one concept relative to another since not all of the subsystem masses (e.g., radiator mass) are presented (see Gallup 1990) and issues other than mass are not discussed here. Furthermore, the assumptions used in generating the input data for these calculations are not entirely consistent.

Several observations on Figures 4-1, 4-2, and 4-3 follow:

- Since a number of parameters may be varied within an allowed range, a smooth curve for mass as a function of power is not always obtained; however, for illustrative purposes a smooth curve was drawn between the scatter in the calculated data points.

- For the LMR, the reactor and shield mass is almost linear over much of the power range (Figure 4-1).

- The TFE reactor mass increases rapidly as the power level increases from 5 to 10 kWe, then increases more gradually up to 350 kWe (Figure 4-2). The change in the TFE reactor mass slope may be due in part to the selection of a moderated TFE concept at 10 kWe rather than a driver fuel concept, which was chosen for the 5-kWe case. As explained in Section 2.2, the concept selected at each power level is based on minimizing the overall system mass. At 100 kWe and above, an all-TFE concept yields the minimum system mass.

- Since the OTR reactor mass increases rapidly at high power, the OTR mass predictions are presented at power levels equal to and less than 50 kWe.

Component mass and dimensional estimates are presented as examples for 100-kWe LMR and TFE concepts in Tables 4-1 and 4-2, respectively; mass and dimensional data for a 5-kWe

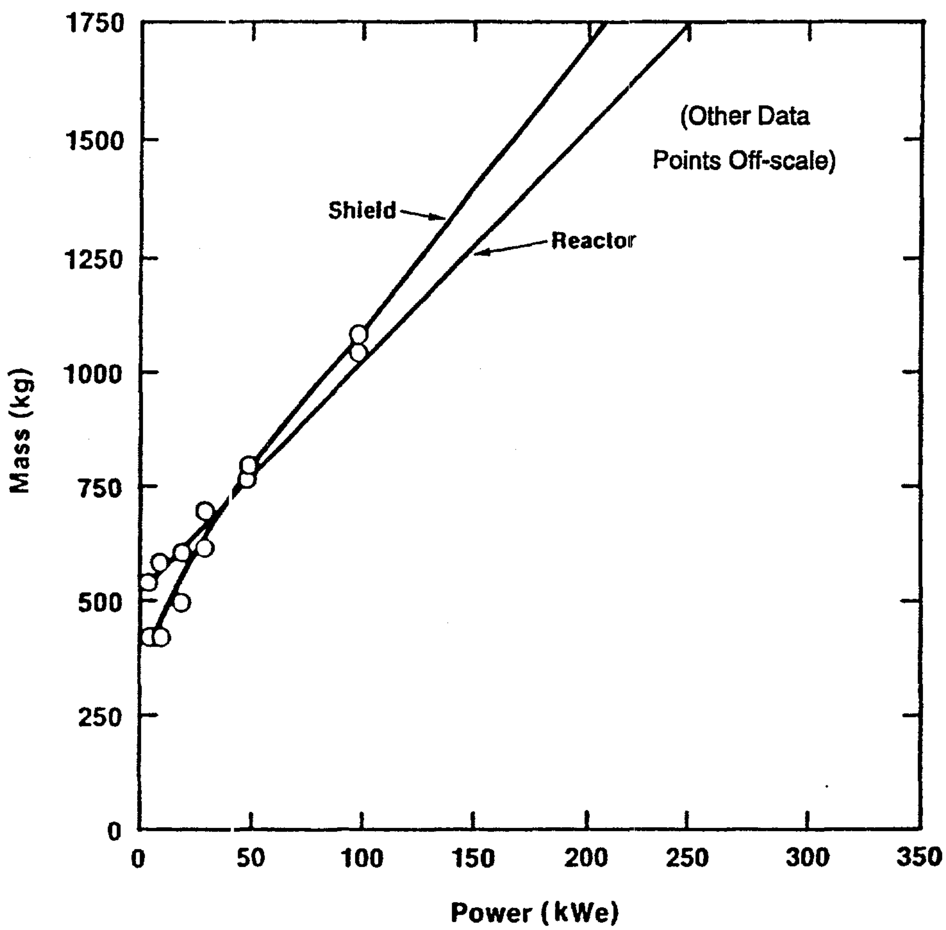

Figure 4-1. RSMASS-D estimated reactor and shield masses for the LMR.

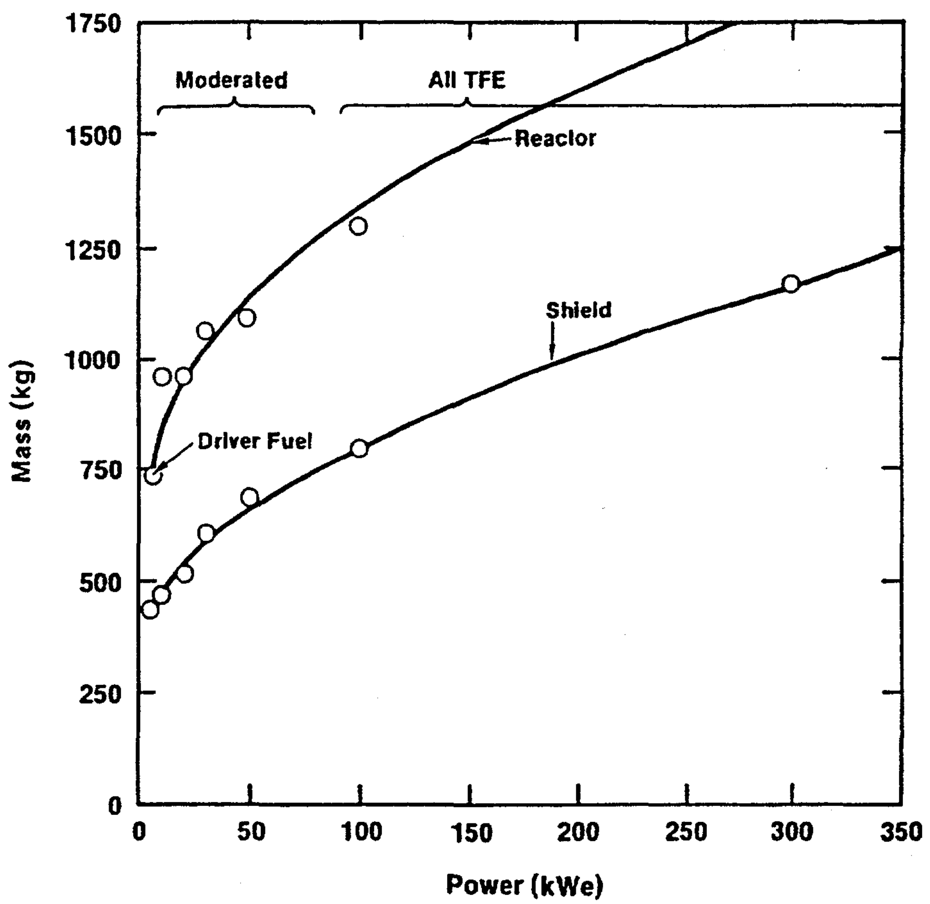

Figure 4-2. RSMASS-D estimated reactor and shield masses for the in-core thermionic reactor.

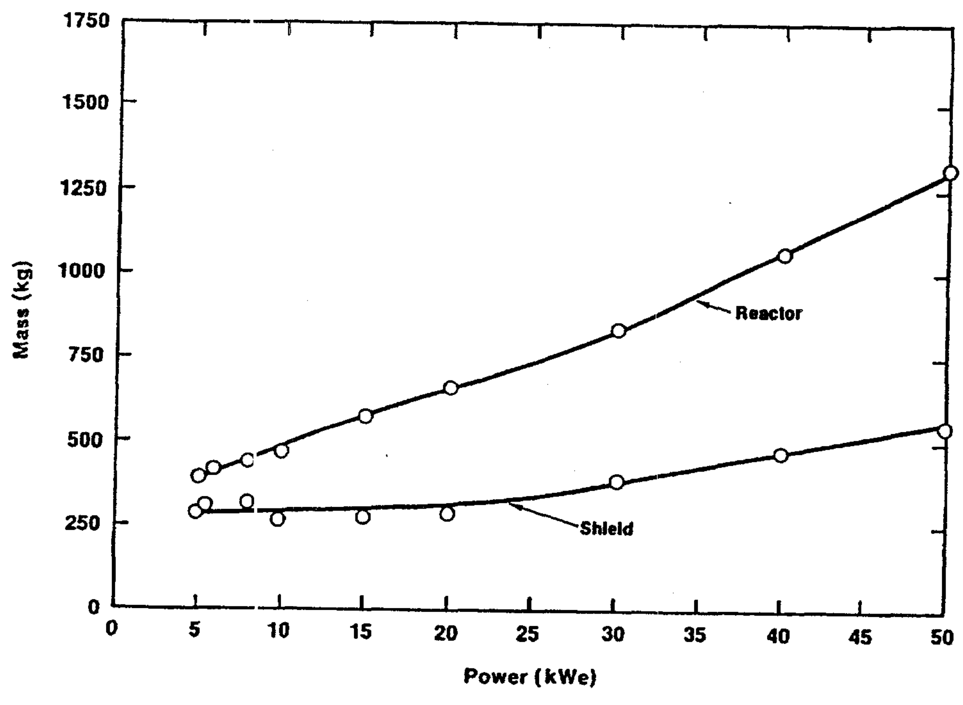

Figure 4-3. RSMASS-D estimated reactor and shield masses for the OTR.

Table 4-1. 100-kWe LMR Mass and Dimensional RSMASS-D Estimates

OPTIMIZED MASS SUMMARY		
Reactor		
Fuel	166 kg	
Reflector	184 kg	
Pressure vessel	70 kg	
Structure	141 kg	
Total		561 kg
I&C		255 kg
Safety systems		
Reentry shield	25 kg	
Rods and drives	75 kg	
Auxilliary cooling	48 kg	
Loop and		
Rhenium liner		
Total		148 kg
Shield		
Neutron	375 kg	
Gamma	422 kg	
Beryllium	147 kg	
Total		945 kg
OPTIMIZED DIMENSIONAL SUMMARY		
Reactor core		
Length	39.6 cm	
Core diameter	31.2 cm	
Reflector thickness	9.7 cm	
Total volume		0.26 m^3
Shield		
Neutron thickness	57.8 cm	
Gamma thickness	5.0 cm	
Be thickness	7.0 cm	
Front diameter	118.5 cm	
Total volume		0.53 m^3

Table 4-2. 5-kWe TFE Mass and Dimensional RSMASS-D Estimates

OPTIMIZED MASS SUMMARY		
Reactor		
Fuel	27 kg	
Reflector	93 kg	
Pressure Vessel	23 kg	
Structure	190 kg	
Total		333 kg
Shield		
Neutron	116 kg	
Gamma	321 kg	
Beryllium	0 kg	
Total		437 kg
OPTIMIZED DIMENSIONAL SUMMARY		
Reactor Core		
Length	37.5 cm	
Core diameter	30.3 cm	
Reflector thickness	7.4 cm	
Total volume		0.15 m^3
Shield		
Neutron thickness	40.6 cm	
Gamma thickness	28.5 cm	
Front diameter	61.4 cm	
Total volume		0.19 m^3

OTR are presented in Table 4-3. In general, the component masses and dimensions appear to be quite reasonable. Care should be exercised when comparing these estimates with any detailed calculated results, since the design and operational assumptions used for these RSMASS-D calculations may not be consistent with the assumptions for the detailed calculations.

4.2 Comparison with Detailed Calculations

RSMASS-D mass estimates have been compared with mass projections for all three reactor and shield models. The results below show that RSMASS-D fulfills its accuracy goal of ± 20 percent of the mass predicted by detailed calculations. This accuracy goal is for comparisons in which both RSMASS-D and the detailed calculations use the same design and operational assumptions. Different design assumptions (such as pin diameter, fuel temperature) and the components included in the mass tally can have a significant impact on mass.

4.2.1 LMR Comparison

The results of the LMR comparison are provided in Table 4-4. The LMR detailed calculations were obtained from a GE viewgraph presentation (GE, 1988b) for a 100-kWe system. As the results in Table 4-4 show, the RSMASS-D predictions for reactor (including contributions from safety instrumentation and control subsystems) and shield mass are within 9 and 3 percent, respectively, of the GE-calculated mass. (For this comparison, RSMASS-D used the same assumptions and parameters as in the GE study rather than allowing the code to optimize the design.)

4.2.2 TFE Reactor Comparison

The results of the TFE reactor comparison for a TOPAZ-type TFE reactor with TOPAZ as-built mass data are provided in Table 4-5. The RSMASS-D reactor mass agrees with Russian data (USAF, 1992) within 15 percent, and the shield mass estimate agrees within 12 percent. As with the SP-100 comparison, RSMASS-D was forced to use the same design and operational assumptions as in the actual design.

4.2.3 OTR Comparison

The OTR comparison with detailed calculations (GA, 1987b) is for a 6-kWe system (Table 4-6). The reactor mass, with thermionic devices, estimated by RSMASS-D is within 10 percent of the GA predictions, and the shield mass agrees within 13 percent. As with the LMR and TFE comparisons, consistent assumptions were made for this comparison.

Table 4-3. 5-kWe OTR Mass and Dimensional RSMASS-D Estimates

OPTIMIZED MASS SUMMARY		
Reactor		
Fuel	75 kg	
Moderator	19 kg	
Structure	19 kg	
Reflector	100 kg	
Total		213 kg
I&C		133 kg
Safety systems		
Reentry shield	18 kg	
Rods and drives	39 kg	
Total		57 kg
Shield		
Neutron	137 kg	
Gamma	232 kg	
Total		369 kg
OPTIMIZED DIMENSIONAL SUMMARY		
Reactor Core		
Length	30.7 cm	
Core diameter	26.0 cm	
Reflector thickness	10.0 cm	
Total volume		0.084 m^3
Shield		
Neutron thickness	40.6 cm	
Gamma thickness	16.0 cm	
Be thickness	68.0 cm	
Front diameter	111.1 cm	
Total volume		0.21 m^3

Table 4-4. RSMASS-D LMR Mass Estimate Comparison with Detailed Calculated Mass Predictions[a]

Subsystem	Mass (kg)		Deviation (%)
	RSMASS-D	GE	
Reactor, safety system, and I&C	964	1056	–9
Shield	945	920	+3

[a]From GE (1988b)

Table 4-5. RSMASS-D TFE Mass Estimate Comparison with Detailed Calculated Mass Predictions[a]

Subsystem	Mass (kg)		Deviation (%)
	RSMASS-D	TOPAZ II	
Reactor and I&C	333	290	+15%
Shield	439	390	+12

[a]From USAF (1992)

Table 4-6. RSMASS-D OTR Mass Estimate Comparison with Detailed Calculated Mass Predictions[a]

Subsystem	Mass (kg)		Deviation (%)
	RSMASS-D	GA	
Reactor and Thermionics	243	221	+10
Shield	369	417	–13

[a]From GA (1987b)

THIS PAGE INTENTIONALLY LEFT BLANK

References

Dean, N.A., et al. (1991). "SP-100 Reactor and Shield Design Update," in *8th Symposium on Space Nuclear Power Systems,* M.S. El-Genk and M.D. Hoover, eds., Institute for Space Nuclear Power Studies, University of New Mexico, Albuquerque, NM.

Gallup, D.R. (1990). *The Scalability of OTR Space Nuclear Power Systems,* SAND90-0163, Sandia National Laboratories, Albuquerque, NM.

GA (General Atomics Technologies) (1985). Thermionic Space Power Systems, summary briefing, GA-C17976, Viewgraph presentation, Jet Propulsion Laboratory, Pasadena, CA.

GA (General Atomics Technologies) (1987a). "Concept Definition Phase of the STAR-C Thermionic Power System for the Boost Surveillance and Tracking System," GA-C18676, San Diego, CA.

GA (General Atomics Technologies) (1987b). Moderated In-Core Thermionic Space Reactors, Presentation to DOE/USAF small space reactors review panel.

GA (General Atomics Technologies) (1989). "TFE Verification Program Semiannual Report for the Period Ending April 30, 1989," GA-A1966, San Diego, CA.

GE (General Electric Co.), (1983). SP-100 Derivative Small Space Reactor Power Systems, Briefing to USAF/DOE Evaluation panel for small space reactor systems, Los Angeles, CA.

GE (General Electric Co.) (1988a). SP-100 GE project integration meeting, Viewgraph presentation, Jet Propulsion Laboratory, Pasadena, CA.

GE (General Electric Co.) (1988b). SP-100 Reference Flight System: System Design Review, Viewgraph presentation, Valley Forge, PA.

Marshall, A.C. (1986). *RSMASS: A Preliminary Reactor/Shield Mass Model for SDI Applications,* SAND86-1020, Sandia National Laboratories, Albuquerque, NM.

Marshall, A.C. (1989). "Further Improvements to the STAR C Shield Model," memorandum to L. Cropp, April 4.

Marshall, A.C., and B. McKissok (1990). "Scaling Study for SP-100 Reactor Technology," in *Seventh Symposium on Space Nuclear Power Systems*, M.S. El-Genk and M.D. Hoover, eds., pp. 132–139, Institute for Space Nuclear Power Studies, University of New Mexico, Albuquerque, NM.

Marshall, A.C, and D.R. Gallup (1991). "RSMASS-D: Reactor and Shield Mass Minimization Models," in *Eighth Symposium on Space Nuclear Power Systems*, M.S. El-Genk and M.D. Hoover, eds., pp. 228–233, American Institute of Physics Press, New York.

McDaniel, R., and J. M. Harris (1983). "A Theoretical Analysis of the Effect of Thermal Neutron Absorbers on Dual Detector Porosity Log Measurements," in *ANS Transactions*, Vol. 45, pp. 217-218.

Merril, M. (1986). General Atomics Technologies staff member, personal communication, March.

Murata, R. (1988). General Electric staff member, personal communication, June 10.

Sholtis, J.A. Jr., et al. (1994). "U.S. Space Nuclear Safety: Past, Present, and Future," in *A Critical Review of Space Nuclear Power and Propulsion 1984-1993*, J.H. El-Genk, ed., pp. 269-303, American Institute of Physics Press, New York.

SPI (Space Power, Inc.) (1987a). SNAP/TOPAZ Program Derivative Small Reactor Space Power System 10 kWe/30 kWe, presentation to DOE/Air Force small reactor committee, Space Powerline, Aerospace Corp., Los Angeles, CA.

SPI (Space Power, Inc.) (1987b). MMWe Space Power System Concept Report, SPS-19-1, San Jose, CA.

USAF (1992). TOPAZ CoDR, Phillips Laboratory presentation at the TOPAZ-II conceptual design review, Albuquerque, NM.

Appendix A: Reactor Geometry Correction Factor

A simple formula [see Equations (2.1-4), (2.2-15), and (2.3-8)] has been developed to account for the fact that the reactor is a cylinder rather than a sphere, and that the length-to-diameter ratio, *a*, may be greater than 1.0. The derivation of this formula is presented in the following:

$$k_{\text{eff}} = \frac{k_\infty}{1+M^2B^2}, \qquad \text{(A-1)}$$

where k_{eff} is the effective neutron multiplication factor, k_∞ is the infinite medium multiplication factor, $M^2$is the migration area, and B^2 is the reactor buckling.

For a critical reactor, k_{eff} must equal 1.0. Since the reactor materials are the same for the cylindrical and spherical cases, it follows that

$$k_\infty^{CL} = k_\infty^{SP} \text{ and } M_{CL}^2 = M_{SP}^2,$$

where *CL* designates cylinder and *SP* designates sphere. Using the information in Equation (A-1), the following can be obtained:

$$B_{CL}^2 = B_{SP}^2. \qquad \text{(A-2)}$$

It is known that

$$B_{CL}^2 = \left[\frac{2.405}{r_{CL}}\right]^2 + \left[\frac{\pi}{H_{CL}}\right]^2 \qquad \text{(A-3)}$$

and

$$B_{SP}^2 = \left[\frac{\pi}{r_{SP}}\right]^2, \qquad \text{(A-4)}$$

where r is radius and H is core height. Core height can be expressed as

$$H_{CL} = 2r_{CL}a, \tag{A-5}$$

where a is core length/core diameter.

Then, substituting (A-5) into (A-3) and (A-3) and (A-4) into (A-2) yields

$$\left[\frac{2.405}{r_{CL}}\right]^2 + \left[\frac{\pi}{2ar_{CL}}\right]^2 = \left[\frac{\pi}{r_{SP}}\right]^2. \tag{A-6}$$

By transposing terms, the following is obtained:

$$r_{CL} = \frac{r_{SP}}{2a}[2.34a^2 + 1]^{1/2} \tag{A-7}$$

The ratio of critical masses is given by

$$\frac{M_{CL}}{M_{SP}} = \frac{\pi r_{CL}^2 H}{\frac{4}{3}\pi r_{SP}^3} = \frac{2\pi r_{CL}^3 a}{\frac{4}{3}\pi r_{SP}^3}, \tag{A-8}$$

and (A-7) can be substituted into (A-8) to obtain

$$\frac{M_{CL}}{M_{SP}} = \frac{0.188(2.34a^2 + 1)^{3/2}}{a^2}. \tag{A-9}$$

In Marshall (1986) it was observed that when the effect of the reflector is accounted for, the mass correction must be taken to the two-thirds power, hence:

$$\frac{M_{CL}}{M_{SP}} = \frac{1}{3}(2.34a^{2/3} + a^{-4/3}) \tag{A-10}$$

A comparison of (A-10) with a more elaborate approach (Paxton, 1986) has indicated an accuracy of 2 percent for $a = 1.0$, and an accuracy within 15 percent for $a \geq 2.0$.

References for Appendix A

Paxton, H.C. (1966). *Criticality Control in Operations with Fissile Material,* LA-3366, UC-46, TID-4500, Los Alamos National Laboratory, Los Alamos, NM.

Marshall, A.C. (1986). RSMASS: *A Preliminary Reactor/Shield Mass Model for SDI Applications,* SAND86-1020, Sandia National Laboratories, Albuquerque, NM.

THIS PAGE INTENTIONALLY LEFT BLANK

Appendix B: RSMASS-D Input Parameters

The tables that follow present sample input parameter values for the liquid-metal-cooled reactor (LMR) (Table B-1), the thermionic fuel element (TFE) reactor (Table B-2), and the out-of-core thermionic reactor (OTR) (Table B-3).

Table B-1. Sample LMR Input Parameters

Reactor Input Parameters		
Parameter	Description	Value
P	Electrical power level [MWe].	0.10
t	Operating time [years].	7.0
ε	Fractional fuel enrichment.	0.97
e	Net fractional efficiency.	0.042
M_{CR}	Reference critical mass [kg].	150
C_m	Critical mass correction factor.	1.0
r_{oc}(min)	Minimum fuel pin radius [m].	3.8×10^{-3}
r_{oc}(max)	Maximum fuel pin radius [m].	1.25×10^{-2}
Nr_{oc}	Number of intervals between r_{oc} (min) and r_{oc} (max).	5
a(min)	Minimum aspect ratio for core.	1.0
a(max)	Maximum aspect ratio for core.	2.0
N_a	Number of intervals between a(min) and a(max).	6
SD(min)	Minimum smear density (fraction of theoretical).	0.80
SD(max)	Maximum smear density.	1.0
NSD	Number of intervals between SD(min) and SD(max).	6
P_F	Peak/average core power.	1.52
ρ_F	Fuel density [kg/m^3].	13730
k	Gap gas thermal conductivity [W/mK].	0.46
k_f	Fuel thermal conductivity [W/mK].	26.0
k_{Lc}	Liner/cladding thermal conductivity [W/mK].	52.0
h_c	Coolant heat transfer coefficient [W/m^{2}K].	4.0×10^4
T_f	Maximum allowable fuel temperature [K].	1650

Table B-1. Sample LMR Parameters (Concluded)

Reactor Input Parameters (Continued)		
Parameter	Description	Value
T_c	Maximum coolant temperature [K].	1350
T	Reflector thickness [m].	0.10
ρ_{Rf}	Reflector density [kg/m^3].	3000
F_{rp}	Multiplier to get pressure vessel radius.	1.09
F_{Lp}	Multiplier to get pressure vessel length.	1.40
n	Pressure vessel locator.	0
P_r	Reactor coolant pressure [MPa].	0.15
U_s	Pressure vessel strength [MPa].	280.0
ρ_{pv}	Pressure vessel density [kg/m^3].	8570
t_{min}	Minimum pressure vessel thickness [m].	2×10^{-3}
d_1	Constant I&C mass [kg].	126
d_2	Proportionality constant for control mass [kg/m^2].	707
d_3	Proportionality for cable mass [kg/m].	2.7
Shield Input Parameters		
D_g	Maximum allowed payload gamma dose [rem].	5×10^5
D_n	Maximum allowed payload neutron dose [nvt].	1×10^{13}
R_p	Payload separation distance [m].	22.5
D_{pay}	Payload diameter [m].	4.0
$t_{g\ min}$	Minimum gamma shield thickness [m].	0.02
$t_{g\ max}$	Maximum gamma shield thickness [m].	0.09
N_g	Number of gamma shield thicknesses.	15
F_{BM}	Boom mass constant [kg/m].	9.0

Table B-2. Sample TFE Reactor Input Parameters

Reactor Input Parameters		
Parameter	Description	Value
P	Electrical power level [MWe].	0.05
t	Operating time [years].	7.0
ε	Fractional fuel enrichment.	0.97
C_m	Critical mass correction.	1.0
e_T	Fractional TFE efficiency.	0.084
r_e (min)	Minimum emitter outer radius [m].	5×10^{-3}
r_e (max)	Maximum emitter outer radius [m].	1.5×10^{-2}
Nr_E	Number of emitter radii to be considered.	5
a(min)	Minimum aspect ratio for core.	1.0
a(max)	Maximum aspect ratio for core.	2.0
N_a	Number of aspect ratios to be considered.	6
T_m (min)	Minimum moderator thickness [m].	0.0
T_m (max)	Maximum moderator thickness [m].	0.014
N_{Tm}	Number of moderator thicknesses to be considered.	8
U_{LD} (min)	Minimum driver region uranium loading [wt %].	0.0
U_{LD} (max)	Maximum driver region uranium loading [wt %].	17.0
N_{ULD}	Number of uranium loadings to be considered.	6
ϕ	Maximum electrical power flux [MW/m^2].	6.8
ρ_{fT}	Fuel pellet density in TFE [kg/m^3].	1.0×10^4
P_{FT}	Peak-to-average power ratio in TFE fuel.	1.40
P_{fD}	Peak-to-average power ratio in driver fuel.	1.40
β_T	Maximum allowed fuel burnup fraction in TFE.	0.10
β_D	Maximum allowed fuel burnup fraction in driver.	0.10
Z	Fuel pellet outer diameter/inner diameter.	4.0
k_f	Fuel thermal conductivity [W/mK].	2.6
T_f	Maximum allowed fuel temperature [K].	2200

Table B-2. Sample TFE Reactor Input Parameters (Concluded)

Reactor Input Parameters (Continued)		
Parameter	Description	Value
T_e	Maximum allowed emitter temperature [K].	1800
ρ_M	Moderator density [kg/m^3].	5610
ρ_{ST}	TFE region structure density [kg/m^3].	4880
ρ_{SM}	Moderator region structure density [kg/m^3].	1300
ρ_{Rf}	Reflector density [kg/m^3].	3000
T	Reflector thickness [m].	0.10
F_{rp}	Multiplier to get pressure vessel radius.	1.10
F_{Lp}	Multiplier to get pressure vessel length.	2.00
n	Pressure vessel locator.	0
P_r	Reactor coolant pressure [MPa].	0.20
U_s	Pressure vessel strength [MPa].	280
ρ_{pv}	Pressure vessel density [kg/m^3].	8570
t_{min}	Minimum pressure vessel thickness [m].	2×10^{-3}
d_1	Constant I&C mass [kg].	126
d_2	Proportionality constant for control mass [kg/m^2].	707
d_3	Proportionality constant for cable mass [kg/m].	2.7
Shield Input Parameters		
D_g	Maximum allowed payload gamma dose [rem].	5×10^5
D_n	Maximum allowed payload neutron dose [nvt].	1×10^{13}
R_p	Payload separation distance [m].	22.5
D_{pay}	Payload diameter [m].	4.0
t_{gmin}	Minimum gamma shield thickness [m].	0.20
t_{gmax}	Maximum gamma shield thickness [m].	0.80
N_g	Number of gamma shield thicknesses.	15
F_{BM}	Boom mass constant [kg/m].	9.0

Table B-3. Sample OTR Input Parameters

Reactor Input Parameters		
Parameter	Description	Value
P	Electrical power level [MWe].	5×10^{-3}
E	Total lifetime electrical energy [MWe].	7
ε	Fractional fuel enrichment.	0.97
e	Net fractional efficiency.	13.3
β	Fractional burnup limit.	0.01
ϕ	Maximum electrical power flux [MW/m^2].	8.5
f_e	Fraction of core surface area available for thermionics.	0.8
a(min)	Minimum aspect ratio [length/diameter] for core.	1.0
a(max)	Maximum aspect ratio [length/ diameter] for core.	2.5
a_{na}	Number of intervals between a(min) and a(max).	11
b(min)	Minimum ratio of fuel inside diameter to core outer diameter.	0.3
b(max)	Maximum ratio of fuel inside diameter to core outer diameter.	0.7
b_{na}	Number of intervals between b(min) and b(max).	2.0
α	Ratio of fuel annulus outer diameter to core total diameter.	0.93
C_m	Critical mass correction factor.	1.10
VF_{fF}	Volume fraction of fuel in the fuel annulus.	0.50
VF_{fM}	Volume fraction of moderator in the fuel annulus.	0.50
ρ_F	Fuel density [kg/m^3].	11800
ρ_M	Moderator density [kg/m^3].	1850
d_1*	Constant I & C mass [kg].	79
d_2	Proportionality constant for control mass [kg/m^2].	707
d_3*	Proportionality constant for cable mass [kg/m].	0.9
T_f	Maximum allowed fuel temperature [K].	2300
T_{cs}	Core surface temperature [K].	2020
P_F	Peak/average core power factor.	1.20
k_f	Fuel region thermal conductivity [W/mK].	35.0

*A coolant is not required for the OTR instrumentation, and I&C cable mass will be less than for the LMR or TFE concepts.

Table B-3. Sample OTR Input Parameters (Concluded)

Reactor Input Parameters (Continued)		
Parameter	Description	Value
ρ_s	Structural density [kg/m^3].	0.0
T	Reflector thickness [m].	0.10
ρ_{Rf}	Reflector density [kg/m^3].	1470
D_g	Maximum allowed payload gamma dose [rem].	5×10^5
D_n	Maximum allowed payload neutron dose [nvt].	1×10^{13}
R_p	Payload separation distance [m].	15
D_{pay}	Payload diameter [m].	4.0
$t_{g\ \text{min}}$	Minimum gamma shield thickness [m].	0.10
$t_{g\ \text{max}}$	Maximum gamma shield thickness [m].	0.20
N_g	Gamma shield thickness increment [m].	11
Other Input Parameters		
U_r	Mass-to-power ratio for radiator [kg/MW].	420
U_t	Mass-to-power ratio for thermionic devices (kg/MW).	7×10^3
F_{BM}	Boom mass constant [kg/m].	9

Appendix C: Shield Model Attenuation Coefficients

The neutron and gamma attenuation coefficients, A_n and A_g, respectively, are referred to in Section 3 for the shield mass calculations. A_n and A_g were determined by performing spherical transport calculations with the FEMP code. The core is modeled as a homogeneous sphere, and the reflector, the gamma shield, and the neutron shield are modeled as concentric shells. Calculations were first performed for the reference SP-100 reactor described in Section 2.0. Transport calculations were then performed for a variety of shield thicknesses, core materials, and shield materials. The ratio of the dose at some dose plane for the case of interest relative to the dose for the reference case is the value of A_g or A_n for that case.

The results from the transport calculations are obtained as the dose at the outer surface of the shield. Since the shield thickness is not constant, the calculated dose will include the effects of both geometric attenuation and attenuation due to shield interactions. Only the interaction attenuation is desired; consequently, the geometric attenuation must be factored out. If a spherical surface source is assumed, and the point kernel is integrated over the surface of the sphere, it can be shown that the value of the attentuation coefficients are:

$$A_g = \frac{2.63 \times 10^{-12} D_g r_0}{\left[\ln(r_0 + 9.85) - \ln(r_0 - 9.85)\right]}$$

and

$$A_n = \frac{2.42 \times 10^{-17} D_n r_0}{\left[\ln(r_0 + 9.85) - \ln(r_0 - 9.85)\right]},$$

where r_0 is the distance from the core center to the dose plane and D_g and D_n are the doses at the shield surface for gammas and neutrons, respectively.

This correction has been carried out for all the dose calculations used to obtain A_g and A_n. The A_g and A_n matrixes for the LMR, TFE fast, TFE thermal, and OTR reactors are pesented in Tables C-1 through C-8.

Table C-1. A_g for LMR Reactors

t_g(m)	t_n(m)				
	0.0	0.2	0.4	0.6	0.8
0.0	84.4	74.8	59.8	42.0	27.8
0.02	31.6	12.7	10.5	7.67	5.27
0.04	8.94	3.17	2.5	1.88	1.28
0.06	4.13	0.873	0.684	0.499	0.341
0.08	2.79	0.312	0.226	0.168	0.116
0.10	2.23	0.168	0.111	0.836	0.0595

Table C-2. A_n for LMR Reactors

t_g(m)	t_n(m)				
	0.0	0.2	0.4	0.6	0.8
0.0	1.49E6	5820	60.5	0.753	0.00992
0.02	6.6E5	4110	39.3	0.468	0.00605
0.04	5.74E5	3060	26.3	0.294	0.00372
0.06	5.04E5	2360	18.1	0.187	0.00229
0.08	4.4E5	1860	12.7	0.12	0.00141
0.10	3.81E5	1490	9.16	0.0785	0.00088

Table C-3. A_g for TFE Fast Reactors

t_g(m)	t_n(m)					
	0.0	0.2	0.4	0.6	0.8	1.0
0.0	163	160	121	79.9	49.4	30.8
0.2	6.38	5.3	3.71	2.42	1.53	0.0
0.4	0.223	0.18	0.124	0.081	0.0	0.0
0.6	0.008	0.00615	0.00422	0.0	0.0	0.0
0.8	0.00023	0.00021	0.0	0.0	0.0	0.0
1.0	9.65E-6	0.0	0.0	0.0	0.0	0.0

Table C-4. A_n for TFE Fast Reactors

t_g(m)	t_n(m)					
	0.0	0.2	0.4	0.6	0.8	1.0
0.0	3.38E6	1.94E4	209	2.61	0.034	0.000
0.2	2.51E4	222	2.72	0.0351	0.00045	0.0
0.4	275	281	0.00046	0.0	0.0	0.0
0.6	3.47	0.0367	0.00046	0.0	0.0	0.0
0.8	0.08	0.000477	0.0	0.0	0.0	0.0
1.0	0.000591	0.0	0.0	0.0	0.0	0.0

Table C-5. A_g for TFE Thermal Reactors

t_g(m)	t_n(m)					
	0.0	0.2	0.4	0.6	0.8	1.0
0.0	244	241	179	117	72.9	44.7
0. 2	8.41	7.23	5.05	3.3	2.1	0.0
0.4	0.308	0.251	0.173	0.113	0.0	0.0
0. 6	0.0112	0.00863	0.00591	0.0	0.0	0.0
0.8	0.0004	0.00029	0.0	0.0	0.0	0.0
1.0	1.36E-5	0.0	0.0	0.0	0.0	0.0

Table C-6. A_n for TFE Thermal Reactors

t_g(m)	t_n(m)					
	0.0	0.2	0.4	0.6	0.8	1.0
0.0	1.97E6	1.09E4	125	1.62	0.212	2.75E-4
0.2	1.41E4	1.34	1.68	.0219	3.84E-4	0.0
0.4	166	1.74	.0222	2.86E-4	0.0	0.0
0.6	2.15	0.023	2.9E-4	0.0	0.0	0.0
0.8	0.0284	3.0E-4	0.0	0.0	0.0	0.0
1.0	3.7E-4	0.0	0.0	0.0	0.0	0.0

Table C-7. A_g for OTR Reactors

t_g(m)	t_n(m)					
	0.0	0.2	0.4	0.6	0.8	1.0
0.0	196	194	147	96.5	60.4	37.1
0.2	7.53	6.36	4.43	2.9	1.83	0.0
0.4	0.268	0.217	0.150	0.098	0.0	0.0
0.6	0.00968	0.00743	0.0051	0.0	0.0	0.0
0.8	3.4E-4	2.5E-4	0.0	0 0	0 0	0 0
1.0	1.17E-5	0.0	0.0	0.0	0.0	0.0

Table C-8. A_n for OTR Reactors

t_g(m)	t_n(m)					
	0.0	0.2	0.4	0.6	0.8	1.0
0.0	3.13E6	1.79E4	194	2.42	0.0316	4.1E-4
0.2	2.33E4	206	2.53	0.0327	4.21E-4	0.0
0.4	256	2.61	0.0331	4.25E-4	0.0	0.0
0.6	3.23	0.0343	4.8E-4	0.0	0.0	0.0
0.8	0.0423	4.45E-4	0.0	0.0	0.0	0.0
1.0	5.5E-4	0.0	0.0	0.0	0.0	0.0

Appendix D: Definition of Variables

Table D-1. Definition of Variables

Variable Name	Definition
a	Aspect ratio (core length-to-diameter ratio).
A	Effective core area [m^2].
A_T	Core surface area required for thermionics [m^2].
A_g	Attenuation parameter for deviations from reference conditions.
A_f	Unit cell fuel area for pins on a hexagonal pitch [m^2].
A_h	Total cell fuel area for pins on a hexagonal pitch [m^2].
A_n	Required neutron attenuation.
A_R	Attenuation reduction factor.
A_T	Required thermionic emitter surface area [m^2].
b	Ratio of the inner diameter of the fuel to the outer diameter of the core region, for an OTR.
B	Buildup factor.
B_{CL}^2	Buckling for a cylinder [cm^{-2}]
B_{sp}^2	Buckling for a sphere [cm^{-2}]
C	Combined correction factor for the aspect ratio and miscellaneous effects used for calculating critical mass.
C_a	Correction factor for a core with cylindrical geometry and an aspect ratio of a.
C_m	Correction factor for other (miscellaneous) effects on the critical mass.
C_s	Square root of the smear density of the fuel divided by 0.96.
d_1	Mass of the fixed instrumentation and control (I&C) component [kg].
d_2	Areal density of the size-dependent I&C component [kg/m^2].
d_3	Mass/length of the I&C cables [kg/m].
D	Core diameter [m].
D_g	Gamma dose at the payload from the reactor [rem].
D_{gs}	Gamma dose at the shield outer surface.
D_n	Neutron dose [n/cm^2].
D_{ns}	Neutron dose at the shield outer surface [n/cm^2].
D_{pay}	Payload diameter [m].

Table D-2. Definition of Variables (Continued)

Variable Name	Definition
e	Net fractional efficiency.
e_R	Total TFE reactor fractional efficiency.
e_T	Thermionic efficiency.
E	Electrical energy at the payload [MWe].
f_e	Maximum fraction of the core surface area available as emitter surface.
F_{BM}	Proportionality constant for boom mass.
F_{Lp}	Total pin length multiplier.
F_{rp}	Core radius multiplier.
h_c	Coolant heat transfer coefficient [W/m^{2}K].
k	Thermal conductivity of helium fill gas [W/mK].
k_f	Fuel thermal conductivity [W/mK].
k_g	Fuel/cladding gap effective thermal conductivity [W/mK].
k_c	Thermal conductivity of the graphite annulus [W/mK].
k_{Lc}	Liner cladding thermal conductivity [W/mK].
L	Core length [m].
L_p	Plenum length [m].
L_{pv}	Pressure vessel length [m].
L_s	Distance from the unshielded end of the pressure vessel to the first gamma shield interface [m].
M_B	Fuel mass required for burnup [kg].
M_{Be}	Beryllium shield mass [kg].
M_{BD}	Quantity of uranium burned up in the driver fuel region [kg].
M_{BM}	Boom mass [kg].
M_{BT}	Quantity of uranium burned up in the TFE region [kg].
M^2	Migration area.
M_C	End-of-life critical mass [kg].
M_c^0	Initial critical mass [kg].
M_c^C	Compacted critical mass of ^{235}U [kg].
M_{cD}	The end-of-life critical mass for the driver fuel [kg].

Table D-1. Definition of Variables (Continued)

Variable Name	Definition
M_{cD}^{0}	Initial critical mass required for the driver fuel region [kg].
M_{cD}^{C}	Driver fuel component of the compacted critical mass [kg].
M_{cT}^{c}	Critical mass of the TFE fuel
M_{CR}	Reference critical mass [kg].
M_{CS}	Mass of the conical shield [kg].
M_{cT}	The end-of-life critical mass for the TFE fuel [kg].
M_{cT}^{0}	Initial required critical mass for the TFE fuel region [kg].
M_{E}	Total required end-of-life fuel mass based on neutronics limits [kg].
M_{ED}	The required end-of-life fuel mass based on neutronics for the driver region [kg].
M_{ET}	The required end-of-life fuel mass based on neutronics for the TFE region [kg].
M_{F}	Fuel mass based on burnup (fuel damage) limits [kg].
M_{FD}	Driver fuel mass based on burnup (fuel damage) limits [kg].
M_{FT}	TFE fuel mass based on burnup (fuel damage) limits [kg].
M_{gs}	Gamma shield mass [kg].
M_{HS}	Total heat shield mass [kg].
M_{IC}	The instrumentation and control (I&C) mass [kg].
M_{L}	Actual (limiting) required fuel mass [kg].
M_{LC}	Lithium coolant mass in the reactor [kg].
M_{M}	Moderator mass [kg].
M_{MS}	Miscellaneous safety system mass [kg].
M_{ns}	Neutron shield mass [kg].
M_{NC}	Heat shield nose cone mass [kg].
M_{NK}	Total NaK coolant mass [kg].
M_{p}	Fuel mass based on thermal limits [kg].
M_{pv}	Pressure vessel mass [kg].
M_{R}	The total reactor mass [kg].

Table D-1. Definition of Variables (Continued)

Variable Name	Definition
M_{RAD}	Radiator mass [kg].
M_{Rf}	Total reflector mass [kg].
M_s	Total structural mass [kg].
M_{SET}	The mass of the OTR thermionic devices (known as SET devices) [kg].
M_{SR}	Mass of the safety rod system [kg].
M_{SS}	Total safety system mass [kg].
M_T	Moderator plus fuel mass [kg].
M_{Th}	Total fuel mass based on thermionic and thermal considerations [kg].
M_{ThD}	Driver fuel mass based on thermionic considerations [kg].
M_{ThT}	Mass of TFE fuel required based on thermionic and thermal considerations [kg].
M_{TS}	Total shield mass [kg].
n	Pressure vessel locator.
N_{235}	^{235}U atom density assumed to obtain the values of A_n [atoms/barn cm].
N_{og}	Proportionality constant for a reference set of conditions.
N_s	Proportionality constant.
P	Maximum reactor system electrical power [MWe].
P_D	Thermal power in the driver fuel region [MW].
P_F	Core spatial peak/average power factor.
P_{FD}	Peak-to-average power ratio in the driver fuel.
P_{FT}	Peak-to-average power ratio in the TFE fuel.
P_r	Reactor coolant pressure [MPa].
P_s	Maximum allowed specific power [MWth/kg].
p_{SR}	Ratio of the power density in the driver fuel region to the power density in the TFE region.
P_T	Required thermal power in the TFE fuel [MW].
Q"	Total heat flux
r_1	Conic section radius [m].
r_2	Conic section radius [m].

Table D-1. Definition of Variables (Continued)

Variable Name	Definition
r_3	Conic section radius [m].
r_4	Conic section radius [m].
r_c	TFE total unit cell radius [m].
r_D	TFE driver/moderator outer radius [m].
r_e	TFE emitter radius [m].
r_{eff}	Effective core radius [m].
r_f	Solid fuel pellet radius [m].
r_{ic}	Solid fuel pellet cladding inner radius [m].
r_{oc}	Solid fuel pellet cladding outer radius [m].
r_p	TFE effective pin radius [m].
r_{pv}	Pressure vessel radius [m].
r_r	Total reactor radius [m].
r_t	TFE effective cell radius [m].
R	Core-averaged moderator-to-fuel molecular ratio.
R_a	Inner radius at the narrow end of the conical shield [m].
R_b	Outer radius at the narrow end of the conical shield [m].
R_c	Inner radius at the wide end of the conical shield [m].
R_d	Outer radius at the wide end of the conical shield [m].
R_c^T	Coolant volume-adjusted thermal resistance [m^3K/W].
R_f^T	Volume-adjusted thermal resistance of fuel [m^3K/W].
R_g^T	Fuel cladding gap volume-adjusted thermal resistance [m^3K/W].
R_c^T	Volume-adjusted thermal resistance of the outer graphite annulus [m^3K/W].
R_{Lc}^T	Fuel liner/cladding volume-adjusted thermal resistance [m^3K/W].
R_m	Ratio of driver fuel mass to TFE fuel mass.
R_p	Separation distance between the reactor and payload [m].
R_T^T	Total volume-adjusted thermal resistance across the fuel pin [m^3K/W].
SD	Smear density [unitless].
t	Reactor full-power operating time [years].

Table D-1. Definition of Variables (Continued)

Variable Name	Definition
t_s	Shield thickness [m].
t_c	Combined thickness of the bonded cladding and liner [m].
t_g	Gamma shield thickness [m].
t_{gmin}	Minimum gamma shield thickness.
t_{min}	Minimum pressure vessel thickness [m].
t_n	Actual required neutron shield thickness [m].
t_{ng}	Required neutron shield thickness based on gamma dose limits [m].
t_{nn}	Required neutron shield thickness based on neutron dose limits [m].
t_{pv}	Pressure vessel thickness [m].
T	Reflector thickness [m].
T_c	Outlet coolant temperature [K].
T_{cs}	Temperature of the core surface [K].
T_e	Emitter temperature [K].
T_f	Maximum allowable fuel temperature [K].
T_f^c	Calculated maximum fuel temperature [K].
T_m	Thickness of the TFE moderator region [K].
T_{TS}	Total shield thickness [m].
T_0	Distance from core to nearest shield face [m].
U_{LD}	Driver region uranium load [kg].
U_r	Proportionality constant for calculating radiator mass [kg/MW].
U_s	Ultimate strength of the pressure vessel material [MPa].
U_t	Proportionality constant for calculating mass of thermionic devices [kg/MW].
V	Total core volume [m^3].
V_1 - V_2	Conic section volumes [m^3].
V_M	Moderator volume [m^3].
V_R	Total reactor volume [m^3].
V_T	Volume of the TFE region of the core [m^3].

Table D-1. Definition of Variables (Continued)

Variable Name	Definition
VF	Volume fraction of fuel and moderator.
VF_c	Volume fraction of fuel in the TFE unit cell.
VF_{f^F}	Volume fraction of ^{235}U in the annular fuel region.
VF_{f^M}	Volume fraction of moderator in the annular fuel region.
VF_p	Volume fraction of fuel in the TFE pin.
VF_F	Volume fraction of ^{235}U in the core.
VF_M	Volume fraction of moderator in the core.
VF_{SH}	Void fraction for safety hardware in the core.
x	Thickness of the thinnest part of the $ZrH_{1.7}$ shield.
y	Thickness of the thinnest part of the $ZrH_{1.7}$ and LiH shield combined.
Z	Ratio of the outer to inner TFE fuel pellet diameter.
α	Ratio of the fuel annulus outer diameter to the total core diameter.
β	Fraction of the fuel allowed to burn up.
β_D	Burnup limits for the drive fuel.
β_T	Burnup limits for the TFE fuel.
ΔT	Distance from core to outer shield face [m].
ε	Fractional fuel enrichment.
θ	Radiation shield cone half angle.
μ	Gamma attenuation coefficient [m^{-1}].
μ_c	Core self-absorption coefficient [m^{-1}].
ρ_{fD}	TFE driver region fuel density [kg/m^3].
ρ_{fT}	Density of the TFE fuel [kg/m^3].
ρ_F	Unhomogenized fuel density [kg/m^3].
ρ_{gs}	Gamma shield density [kg/m^3].
ρ_M	Moderator density [kg/m^3].
ρ_{ns}	Neutron shield density [kg/m^3].
ρ_{pv}	Pressure vessel density [kg/m^3].
ρ_{Rf}	Reflector density [kg/m^3].
ρ_S	Density term provided to allow for additional structure [kg/m^3].
ρ_{SM}	Core average density of the moderator/driver region structure [kg/m^3].
ρ_{ST}	Core average density of the TFE region structure [kg/m^3].

Table D-1. Definition of Variables (Continued)

Variable Name	Definition
ρ_T	Moderator plus fuel mass density [kg/m^3].
ϕ	Maximum net electrical power flux at the emitter surface [kg/m^3].

Distribution

Vajislav Banjac
Advanced Technologies Research Corp.
P.O. Box 11218
Albuquerque, NM 87192

Charles Bell
Los Alamos National Laboratory
P.O. Box 1663, MS: K575
Los Alamos, NM 87545

Samit K. Bhattacharyya
Argonne National Laboraotry
9700 South Cass-Bldg. 207
Argonne, IL 60439-4841

Harvey Bloomfield
NASA Lewis Research Center
MS: 301-5
21000 Brookpark Road
Cleveland, OH 44135

Stanley K. Borowski
NASA Lewis Research Center
Adv Space Analysis Office
MS AAC-2
21000 Brookpark Road
Cleveland, OH 44135

Collette Brown
DOE/HQ GTN (MS-NG52)
19901 Germantown Road
Germantown, MD 20585

Niel Brown
5134 Cordoy Lane
San Jose, CA 95124

Glen Cameron
Johns Hopkins University
Applied Physics Laboratory
Building 4, Room 150
Johns Hopkins Road
Laurel, MD 20750-6099

Wade P. Carroll
U.S. Department of Energy
NE-52
19901 Germantown Road
Germantown, MD 20874

Capt Donald R. Culp
DOE/HQ
19901 Germantown Road
Germantown, MD 20874

Lester Begg
General Atomics
P.O. Box 85608
San Diego, CA 92138

Mohamed El-Genk
Institute for Space Nuclear Power Studies
Chemical and Nuclear Engineering
Department
University of New Mexico
Albuquerque, NM 87131

Harold Gerrish
NASA Marshall Space Flight Center
Huntsville, AL 35812

Dave Grant
Applied Physics Laboratory
Johns Hopkins University
Johns Hopkins Road
Laurel, MD 20750-6099

Eric F. Haskin
Institute for Space Nuclear Power Studies
Chemical and Nuclear Engineering Dept.
University of New Mexico
Albuquerque, NM 87131

Mike Houts
Los Alamos National Laboratory
P.O. Box 1663
Los Alamos, NM 87545

James Kee
Booz-Allen & Hamilton, Inc.
Crystal Square 2, Suite 1100
1725 Jefferson Davis Highway
Arlington, VA 22202-4163

Andrew C. Klein
Department of Nuclear Engineering
Oregon State Univerisity
Radiation Center A112
Corvallis, OR 97331-5902

Robert Lange
U.S. Department of Energy
19901 Germantown Road
Germantown, MD 20874

Hans Ludewig
Brookhaven National Laboratory
Building 701
Upton, NY 11719

Jim Mangus
Westinghouse Electric Corporation
Box 158
Madison, PA 15663-0158

John A. Martinell
INEL
P.O. Box 1625
Idaho Falls, ID 83415

Patrick J. McDaniel
PL/WSA
Kirtland AFB, NM 87117-5008

Bill Mehlman
Applied Physics Laboratory
Johns Hopkins University
Johns Hopkins Road
Laurel, MD 20750-6099

Tom Miller
NASA Lewis Research Center
21000 Brookpark Road
Cleveland, OH 44135

Richard L. Moore
U.S. Department of Energy
NE-52
19901 Germantown Road
Germantown, MD 20874

Capt D. Fred Nichols
Defense Special Weapons Agency
GFGA/TAIC
6801 Telegraph Road
Alexandria, VA 22310-3398

James R. Powell
Building 701
Brookhaven National Laboratory
Upton, NY 11973

Norm Roderick
Chemical and Nuclear Engineering Dept.
University of New Mexico
Albuquerque, NM 87131

Lyle Rutger
U.S. Department of Energy
NE-52, GTN
Washington, DC 20585

Glen Schmidt
TOPAZ International Program
901 University Blvd., SE
Albuquerque, NM 87106-4339

Michael J. Schuller
PL/VTPP
Kirtland AFB, NM 87117-5008

Ned Rasor
15601 Montebello Rd.
Cupertino, CA 95015-5404

John M. Smith
NASA Lewis Research Center
MS 301-5
21000 Brookpark Road
Cleveland, OH 44135

Earl Wahlquist DOE/HQ GTWN
MS-NE52
Washington, DC 20545

Carl E. Walter
Lawrence Livermore National Laboratory
MS L-197
P.O. Box 808
Livermore, CA 94550

P. B.Walter
Nuclear Engineering Department
Pennsylvania State University
231 Sackett Building
University Park, PA 16802

Joe Wetch
ISP
621 Riveroaks Parkway
San Jose, CA 95134

Robert Wiley
5998 Camelback Lane
Columbia, MD 21045

Jonathon K. Witter
Department of Nuclear Engineering
Massachusetts Institute of Technology
NW 12-306A
Cambridge, MA 02139

William Determan
Bolling N. American
P.O. Box 7922
Canoga Park, CA 91309-7922

Internal SNL

MS 0835	D. Dobranich, 9113
MS 0425	L. W. Connell, 5415
MS 0425	A. C. Payne, 5415
MS 0719	G. C. Allen, 6131
MS 0720	D. L. Miller, 6804
MS 0722	K. E. Washington, 6534
MS 0727	G. F. Polansky, 6406
MS 0727	D. M. Mulder, 6406
MS 0736	N. R. Ortiz, 6400
MS 0742	C. D. Harmon, 6414
MS 0742	J. E. Kelly, 6414
MS 0744	R. G. Cox, 6402
MS 0744	D. L. Berry, 6403
MS 0744	D. R. Gallup, 6403
MS 0744	M. F. Hessheimer, 6403
MS 0744	D. B. King, 6403
MS 0744	A. C. Marshall, 6403 (20)
MS 0744	F. J. Wyant, 6403
MS 0747	V. J. Dandini, 6412
MS 0748	J. H. Lee, 6413
MS 0767	F. T. Harper, 5514
MS 1003	K S. Kwok, 9602
MS 1139	R. O. Gauntt, 6421
MS 1139	K. O. Reil, 6423
MS 1141	R. L. Coats, 6442
MS 1141	E. J. Parma, 9361
MS 1141	M. E. Vernon, 6441
MS 1142	J. W. Bryson, 9362
MS 1146	R. X. Lenard, 6442
MS 1146	R. Lipinski, 6442
MS 1136	P. S. Pickard, 6440
MS 1146	A. J. Suo-Anttila, 9363
MS 1328	L. C. Sanchez, 6848
MS 1380	M. Berman, 4271
MS 0899	Technical Library, 4916 (5)
MS 0619	Technical Publications, 12690
MS 0619	Review and Approval Desk, 12690 (2) for DOE/OSTI
MS 9018	Central Technical Files, 8940-2
MS 0405	W. H. McCulloch, 12333

FCDSWA, Capt. T. Drake
FCDSWA, Capt. D. Goring
FCDSWA, Michael Jacox
FCDSWA, Lt. Col. D. Kristensen
FCDSWA, Roger Lenard
FCDSWA, Capt. K. McClellan
FCDSWA, Maj. T. McKelvey
FCDSWA, LCDR M. Moruo
FCDSWA, Maj. R. Nelson